Published in final edited form as:
Metallomics. 2011 August ; 3(8): 797–815. doi:10.1039/c1mt00042j.

Metal centers in the anaerobic microbial metabolism of CO and CO_2

Güneş Bender, **Elizabeth Pierce**, **Jeffrey A. Hill**, **Joseph E. Darty**, and **Stephen W. Ragsdale**
Department of Biological Chemistry, University of Michigan, Ann Arbor, Michigan 48109-0606, USA. Fax: +1 734-763-4581; Tel: +1 734-615-4621

Güneş Bender: benderg@umich.edu; Stephen W. Ragsdale: sragsdal@umich.edu

Abstract

Carbon dioxide and carbon monoxide are important components of the carbon cycle. Major research efforts are underway to develop better technologies to utilize the abundant greenhouse gas, CO_2, for harnessing 'green' energy and producing biofuels. One strategy is to convert CO_2 into CO, which has been valued for many years as a synthetic feedstock for major industrial processes. Living organisms are masters of CO_2 and CO chemistry and, here, we review the elegant ways that metalloenzymes catalyze reactions involving these simple compounds. After describing the chemical and physical properties of CO and CO_2, we shift focus to the enzymes and the metal clusters in their active sites that catalyze transformations of these two molecules. We cover how the metal centers on CO dehydrogenase catalyze the interconversion of CO and CO_2 and how pyruvate oxidoreductase, which contains thiamin pyrophosphate and multiple Fe_4S_4 clusters, catalyzes the addition and elimination of CO_2 during intermediary metabolism. We also describe how the nickel center at the active site of acetyl-CoA synthase utilizes CO to generate the central metabolite, acetyl-CoA, as part of the Wood-Ljungdahl pathway, and how CO is channelled from the CO dehydrogenase to the acetyl-CoA synthase active site. We cover how the corrinoid iron–sulfur protein interacts with acetyl-CoA synthase. This protein uses vitamin B_{12} and a Fe_4S_4 cluster to catalyze a key methyltransferase reaction involving an organometallic methyl-Co^{3+} intermediate. Studies of CO and CO_2 enzymology are of practical significance, and offer fundamental insights into important biochemical reactions involving metallocenters that act as nucleophiles to form organometallic intermediates and catalyze C–C and C–S bond formations.

(I) Introduction

Every year, about 750 gigatonnes of relatively inert CO_2 undergoes catalytic reactions that convert it into various forms of organic carbon that is combusted by living organisms and converted back to CO_2 through the many reactions of the carbon cycle.[1] Of the 2.6 gigatonnes of carbon monoxide released into the atmosphere every year, most reacts with hydroxyl radical in the trophosphere, while about 10% is removed by microbes,[2,3] which have the ability to interconvert CO and CO_2 through the activity of CO dehydrogenase. This review will focus on the metalloenzymes and on the catalytic metal centers that are involved in the microbial metabolism of CO and CO_2.

There are six known cycles of microbial carbon dioxide fixation,[4,5] which are summarized in Table 1. The Calvin-Benson-Bassham (CBB) cycle is used by plants and algae in addition to cyanobacteria and other eubacterial clades. The enzyme ribulose-1,5-bisphosphate

Correspondence to: Stephen W. Ragsdale, sragsdal@umich.edu.

carboxylase/oxygenase (RubisCO) in this cycle fixes CO_2 into ribulose-1,5-bisphosphate. The other five pathways described are oxygen-sensitive. Three autotrophic CO_2 fixation pathways have recently been discovered in archaea and bacteria by Georg Fuchs and his coworkers. The hydroxypropionate/malyl-CoA and hydroxypropionate/hydroxy-butyrate cycles include the same two CO_2-fixing enzymes: propionyl-CoA carboxylase and acetyl-CoA carboxylase, while the dicarboxylate/4-hydroxybutyrate cycle includes pyruvate synthase and phosphoenolpyruvate carboxylase to incorporate CO_2 into organic carbon. The reductive citric acid cycle involves three CO_2 fixing enzymes, which are also central to the oxidative citric acid (Krebs) cycle. The Wood-Ljungdahl or reductive acetyl-CoA pathway is unusual in that it generates CO as an intermediate and uses complex metal clusters and organometallic intermediates to fix CO and CO_2 into cellular carbon. Because of the focus of this journal on metals, the enzymes of Wood-Ljungdahl pathway and their metallocenter active sites will be the main subjects of this review. This pathway enables strictly anaerobic bacteria to grow autotrophically on CO or CO_2.

This review will open with a broad description of the chemical and physical properties of CO and CO_2 and of the different enzymatic reactions that utilize them. Then, the focus will turn to the enzymes and the metal clusters in their active sites that catalyze transformations of these two molecules. Pyruvate:ferredoxin oxidoreductase (PFOR), which contains thiamin pyrophosphate (TPP) and multiple Fe_4S_4 clusters, is an example of a class of enzymes that catalyze carboxyl group additions and eliminations during intermediary metabolism in all kingdoms of life. The two types of carbon monoxide dehydrogenase (CODH), which can contain a molybdopterin/copper (Mo-Cu-CODH) or nickel–iron–sulfur (Ni-CODH) active site, have the remarkable property of interconverting CO and CO_2. Acetyl-CoA synthase (ACS), which forms a complex with the Ni-CODH, uses a nickel iron–sulfur cluster to catalyze the reaction of CO with two other substrates to generate the central metabolite acetyl-CoA. A CO channel between the CODH and ACS active sites ensures that CO does not escape from the protein during the enzymatic reaction. Linked to ACS is a corrinoid iron–sulfur protein (CFeSP) that uses vitamin B_{12} and a Fe_4S_4 cluster to catalyze a key methyl-transferase reaction involving an organometallic methyl-Co^{3+} intermediate.[6]

(II) Chemical, physical and biological properties of CO and CO_2

(A) Physical properties of CO and CO_2

Both CO and CO_2 are colorless gases, and CO is odorless, whereas CO_2 has a slightly pungent smell.[7,8] CO is toxic to many organisms, and high levels of CO_2 can become toxic in sealed environments. CO shares many properties with H_2, including low solubility, strong reducing potential and high flammability.[9] The solubilities of CO and CO_2, which depend on temperature and partial pressure, are 22.66 ml kg^{-1} (1 mM) and 835 ml kg^{-1} (37.3 mM), respectively, at 20 °C and 1 atm.[7,9] In aqueous solution, CO_2 is in equilibrium with CO_3^{2-} (carbonate) and HCO_3^- (bicarbonate), which are even more soluble than CO_2 itself.[7] Both gases have many industrial uses (especially CO_2 in all of its forms), and they are released to the atmosphere from many industrial applications that lead to the complete and incomplete oxidation of hydrocarbons.[8,9] Although the anthropogenic sources of CO and CO_2 are often emphasized, the contributions of natural sources are significantly larger.[7,9]

(B) Common chemical reactions and industrial uses of CO and CO

As the most oxidized form of carbon, CO_2 is produced by the complete oxidation of organic carbon. CO_2 is inert under normal conditions; however, it becomes more reactive at high temperatures and in the presence of metal catalysts. Gaseous, solid and liquid carbon dioxide have many industrial uses ranging from being used as a chemical feedstock, a refrigerant as

dry ice and as a stimulator of plant growth in greenhouses.[7] CO_2 can react with H_2 to form CO and H_2O, which is the reverse of the water–gas shift reaction. Another important industrial reaction is the Bosch-Meiser process, which involves the reaction of CO_2 with NH_3 to form urea, which has many industrial uses. Much of the industrially produced CO_2 is a by-product of H_2 production from CH_4 related to the steam refining of natural gas or syngas.

Carbon monoxide is two electrons more reduced than CO_2 and is formed during the incomplete combustion of any organic material. Because it is a strong electron donor, it is used as a reducing agent in some reactions with metals. One common industrial synthesis of CO is the steam reforming of natural gas. At high pressures, it forms carbonyl complexes with metals, and is commonly used in well-known synthetic processes to synthesize other chemicals such as formate, acetic acid and methanol. For example, the Monsanto process involves the synthesis of acetic acid from CO and methanol.[8,9]

(C) CO in biology and medical uses

Even though the toxicity of CO has long been known, its function as a signaling molecule and as a potential therapeutic agent is increasingly recognized.[10] In humans, CO is produced from the degradation of heme by heme oxygenase and it is now known to be a signaling molecule in pathways involving guanylate cyclase and mitogen-activated protein kinases (MAPK). The interaction with soluble guanylate cyclase has implicated a role for CO in vascular and smooth muscle relaxation. The anti-inflammatory and anti-apoptotic effects of CO, protective effects of exogenously applied CO during stress, and possible therapeutic uses of CO in organ transplantation, vascular disease, and cancer are current research areas.[10]

(III) CO and CO_2 in the environment

(A) CO and CO_2 levels over earth's history

CO_2 is a greenhouse gas whose atmospheric concentration has increased by 36% since the beginning of the industrial revolution, and is at a current level of ~380 ppm. CO levels over earth's history appear to track the frequency of volcanic emissions tempered by atmospheric chemistry, dropping from ~100 ppm in the early atmosphere to a current level of 35 to 130 ppb, with its highest levels in the Northern Hemisphere.[11] While the lifetime of CO_2 is~250 years, that of CO is only a few months due to its reaction with other chemicals, mainly hydroxyl radical in the troposphere.[12,13]

(B) Sources and sinks of CO and CO_2

There are both natural and anthropogenic sources of CO_2 and CO. These sources include oxidation of methane and other hydrocarbons in the atmosphere, natural decarboxylation and decarbonylation (tetrapyrrole degradation) reactions and fossil fuel usage for generating energy for electricity, transportation and other industrial activities, which all contribute ~12 billion tons of carbon/year to the atmosphere.[3]

The natural sinks for CO_2 are organisms that perform CO_2 fixation. Plants are a good sink for CO_2 since they use it for generating their cell carbon and are able to uptake more CO_2 than they produce. Many different species of aerobic and anaerobic bacteria and archaea also utilize CO_2 or CO as electron acceptors and donors, respectively, and as carbon sources. Microbes in the soil and in the oceans produce and consume CO_2 and CO, and hence play a central role in the carbon cycle. The soil and the oceans respectively absorb ~120 and ~90 billion tons of carbon annually.[14] These fluxes take place with background carbon amounts of 2000 billion tons on land, 38 000 billion tons in the oceans and 730 billion tons in the

atmosphere. The roles of the different types of microbes in the utilization of CO_2 and CO are summarized in Fig. 1. The anaerobic marine sediments and plants in swamps and peatlands soak up CO_2 to form our oil, coal, natural gas and fossil fuel reserves. There are six known CO_2 fixing pathways.[1,5] Plants, cyanobacteria and a variety of other microbes fix CO_2 into cellular mass using the enzyme, ribulose bisphosphate carboxylase (RubisCO) in the Calvin-Benson-Bassham (CBB) cycle (a.k.a Calvin cycle). In addition to photosynthetic bacteria and cyanobacteria, some chemo-lithotrophs and methylotrophs use CO_2 for making cellular biomass using the Calvin cycle. Phosphoribulokinase, which catalyzes the step before RubisCO, is another crucial enzyme in the Calvin cycle. The Calvin cycle is the only known aerobic carbon fixing pathway, all the other pathways being either somewhat sensitive to O_2 or requiring strictly anaerobic conditions. The Wood-Ljungdahl pathway is extremely oxygen-sensitive and relies heavily on complicated metalloclusters that are inactived upon exposure to O_2.

The Wood-Ljungdahl pathway[15–17] (Fig. 2) is proposed to have fueled the emergence of life on earth.[18,19] This pathway is used by anaerobic microbes in a wide range of phyla (acetogens, sulfate reducers, methanogenc archaea) for acetate oxidation or to convert CO or CO_2 plus H_2 into acetyl-CoA, which is used for ATP and cell carbon synthesis. Acetogenic bacteria also couple this metabolic sequence to other pathways like glycolysis to capture reducing equivalents generated during substrate oxidation for the reduction of CO_2 (or CO) to acetyl-CoA. The Wood-Ljungdahl pathway, as shown in Fig. 2, contains a *methyl* (left side) and a *carbonyl* (right side) branch. The methyl branch involves the six-electron reduction of CO_2 to CH_3–H_4folate, by the folate-dependent one-carbon pathway present in all organisms. The carbonyl branch is unique to microbes using the Wood-Ljungdahl pathway and involves the conversion of CH_3–H_4folate, CO_2 and CoA into acetyl-CoA. The carbonyl branch exhibits distinctive mechanistic features, *e.g.*, low-valent metallocenters serving as nucleophiles, enzymebound organometallic intermediates, unique active site metalloclusters, substrate-derived radicals, and channeling of gaseous substrates.

Atmospheric chemistry and uptake by soil bacteria are the major sinks for CO in the atmosphere. Aerobic carboxidotrophic (oxidizing CO at concentrations >1%) and carboxydovoric (using CO at concentrations<1000 ppm) bacteria and anaerobic microbes like acetogens and methanogens are the major CO oxidizers. Typically, the Mo-dependent carboxidobacterial enzymes have high CO affinities and low turnover numbers, while the anaerobic Ni-CODHs have slightly lower affinities and high turnover numbers, giving catalytic efficiencies of up to 10^9 M^{-1} s^{-1}.[20] Oxidation of natural hydrocarbons and CH_4, and other energy-related emissions, such as incomplete combustion in automobile engines contribute to the net accumulation of CO in the atmosphere, especially in urban areas.

(IV) Non-enzymatic, inorganic compounds that catalyze reactions involving CO and CO_2

Many types of inorganic compounds can catalyze reactions involving CO and CO_2. CO is relatively reactive and can ligate to the low valent states of metal centers. There has been great interest in developing catalysts that can reduce the abundant greenhouse gas CO_2 to other products, including methanol and CO.[21] CO is especially valuable because it is used as a synthetic feedstock in some major industrial processes including the Fisher-Tropsch and Monsanto or Cativa processes for conversion of CO into liquid fuels and acetate, respectively. The major difficulty with CO_2 reduction is that most catalysts that rely on one-electron reduction as an intermediate step must overcome highly unfavorable conversion of CO_2 to the anion radical ($CO_2^{\bullet-}$), which has a standard reduction potential (*vs.* SHE at pH 7) of −1.9 V *vs.* SHE.[22] Some of the nonenzymatic catalysts are mimics of the natural reactions, such as the one catalyzed by CODH.[23,24] However, the enzymatic catalyst,

CODH, catalyzes CO_2 reduction at the thermodynamic potential (which is −0.52 V vs SHE), i.e., without an overpotential. The proposed mechanism for CODH, which catalyzes reaction (1), is viewed to be similar to that of the water gas shift reaction (eqn (2)). Similarly, the reaction steps in the synthesis of acetyl-CoA by ACS are similar to those used by the Ru or Ir catalyst during acetate synthesis by the Monsanto and Cativa processes.

$$CO + H_2O \rightarrow CO_2 + 2H^+ + 2e^- \quad (1)$$

$$CO + H_2O \rightarrow CO_2 + H_2 \quad (2)$$

(A) Synthetic analogues of the aerobic Mo-Cu-CODH active site

Mo-Cu-CODHs are found in aerobic bacteria such as *Oligotropha carboxidovorans* and catalyze reaction (1), which has a standard reduction potential (for the reduction of CO_2 to CO) of −0.520 V. The cofactor consists of a molybdenum ion bound to a pterin dithiolene, with additional hydroxide and *oxo* ligands, and a sulfur bridge to a Cu atom (Fig. 3). In a recent report, mimics of this active site were synthesized by reacting thiomolybdates such as $[MoO_2S_2]^{2-}$ with Cu complexes. The synthesized molecules were characterized by UV-VIS spectroscopy and crystallography, and some of them were found to be good structural analogs of the active site of the enzyme.[25] Density functional theory (DFT) calculations on the model compounds representing possible reaction intermediates in the reaction cycle indicate that the bis-oxo form of Mo is the active catalyst.[26] These computations also suggest that an n-butyl-isonitrile-bound structure of the active site observed in the crystal[27] may not represent a structure that is analogous to what would be observed with the substrate, CO, because of the relative instability of this structure when CO is used in the calculations.[26]

(B) Synthetic analogues of the anaerobic Ni-CODH active site

The anaerobic CODHs also catalyze reaction (1). Model complexes have been synthesized that can catalyze either CO oxidation or its reverse. Some of these were synthesized before the active site structure was known by X-ray crystallography, while many of those synthesized afterwards focus on mimicking the $NiFe_3S_4$ fragment and the pendant Fe atom (Fig. 4c).[24] Complexes containing Ni(II) cyclam Cl_2 that can catalyze CO_2 reduction to CO require very negative redox potentials (~−1.0 V).[28] Tetraazamacrocyclic complexes of Ni and Co can catalyze this reaction along with the reduction of protons to H_2, [29] and there are several reports of CO_2 reduction by porphyrins or phthalocyanine with Co and Fe bound.[30–32] A carbene-supported copper boryl complex and other copper complexes also reduce CO_2 and some Cu complexes even reduce CO_2 to methane and ethane.[33,34] Even less complicated inorganic compounds such as TiO_2 and ZrO_2 can catalyze the reduction of CO_2 when excited with certain energies of light.[35] Monometallic and bimetallic Pd complexes exhibit high catalytic rates (up to 10^4 M^{-1} s^{-1}) and low overpotentials (0.1 to 0.3 V) for CO_2 reduction, yet they exhibit only 10–100 catalytic turnovers before the catalyst undergoes deactivation.[36] More recently, a complicated Rhenium complex was used to reduce CO_2 to CO with H_2 as the electron donor.[37]

Some Ni(II) complexes with O-, N- and S-donor ligands can catalyze CO oxidation with methyl viologen as electron acceptor at very low catalytic rates such as ~0.00027 turnovers/s.[38] CO oxidation on Cu oxide related catalysts is another well-studied system due to practical applications such as automative exhaust control, and some systems in cetain conditions are able to convert 90% of CO within minutes.[39,40] Some other research has

looked at the transformation of CO further to formyl, hydroxymethyl and methyl groups on metal rhenium complexes.[21]

Biomimetic model complexes related to CODH composed of cubane-type and cubanoid $NiFe_3S_4$ clusters have been synthesized and characterized by crystallography, redox potentiometry and Mössbauer spectroscopy, but the CO/CO_2 conversion activities of these complexes have not been tested. A cubanoid structure, $[(tdt)NiFe_3S_4(LS_3)]^{3-}$ (where LS_3: a semirigid trithiolate ligand, tdt: toluene-3,4-dithiolate), mimicked the important aspects of the C-cluster, such as the square planar, four-coordinate Ni^{2+} at one corner of the cubanoid, however it lacked the *exo* Fe found in the CODH active site.[41] This work was an extension of earlier studies on the synthesis of cubanoid type clusters with $[NiFe_3S_4]^+$ cores with a planar Ni geometry where it was possible to insert other metals such as Pd^{2+} and Pt^{2+} in place of Ni^{2+}.[42] There have been some recent syntheses of complexes that mimic exclusively the Ni^{2+}-Exo-Fe^{2+} component of the C-cluster.[43]

(C) Inorganic model compounds similar to the A-cluster

Since the discovery of the A-cluster (Fig. 4d), there have been many attempts to synthesize model compounds with similar properties to, or that mimic the different parts of the A-cluster. The review by Riordan gives a succinct survey of the earlier model compounds that were synthesized and analyzed.[45] There have been other excellent reviews of early models of the A-cluster.[24,46] Thioether ligands provide good models in providing electron densities on Ni similar to the one in the protein. A Cys-Gly-Cys peptide has also been used to generate the square planar Ni^{2+} complex, and binuclear derivatives of this complex, such as [(CysGlyCys)Ni]Ni(dppe) (Fig. 5a) have also been synthesized. In these binuclear complexes, the Ni that is equivalent to the Ni_p of the enzyme could undergo two-electron reduction to Ni^0.

Some single Ni(II) compounds with one amine and three thioester donors to Ni, are able to be methylated, react with CO to form acetyl groups, and acetylate thiol substrates.[46] Similarly, early model studies of the Ni_d site revealed some key features such as the square-planar Ni(II) geometry and the very low potentials required for CO_2 reduction. Bi or trinuclear sulfur-bridged Ni complexes have been synthesized and their reduction and reaction with CO were studied. The compound, $[Ni^{II}(dppe)Ni^{II}(PhPepS)]$ (Fig. 5b) showed striking similarity in EPR and IR spectra to ACS when CO was bound in reducing conditions.[46]

Harrop *et al.* synthesized a dinuclear nickel center model (Fig. 5b) with a dicarboxamido–dithiolate ligated Ni_d mimic sulfur-bridged to a Ni(II) center that could be reduced to Ni(I) and bind CO to form a putative six coordinate Ni(I)–CO complex. The IR spectrum of this complex is similar to the Ni(I)–CO band observed with ACS.[48] Riordan's lab also synthesized a dinuclear Ni(II) complex from a Cys-Gly-Cys bound Ni_d site and $(R_2PCH_2CH_2PR_2)$–$NiCl_2$ (Fig. 5a).[47] More recently, single thiolato-bridged binuclear Ni–S–Ni complexes were formed by reacting $Ni(N_2S_2)$ compounds with $(dppe)Ni(CH_3)Cl$, which provided analogues for the methylated A-cluster (Fig. 5c).[49] These compounds had labile Ni–S bonds and are prone to dissociation/religation. An EPR-active Ni(III)-alkyl intermediate was observed and characterized in a distorted trigonal bipyramidal environment, with a model compound mimicking only the Ni_p portion of the A-cluster (Fig. 5d),[50] giving support to the proposed mechanism with high valent Ni(III)–CH_3 or Ni(III)-acetyl intermediates. The Tatsumi lab synthesized analogues of the A-cluster, one of which is shown in Fig. 5e, that can be methylated by methyl-cobaloxime, and that can further react with CO to form an acetylthioester compound similar to acetyl-CoA.[51,52] In these studies, the compound $Ni(dadt^{Et})Ni(Me)(SDmp)$, where $dadt^{Et}$ stands for *N*,*N*′-diethyl-3,7-diazanonane-1,9-dithiolate and Dmp for 2,6-dimesitylphenyl, was synthesized as a Ni^{II}–Ni^{I}

complex. It had a $S = 1/2$ EPR signal ($g_{x,y,z}$ = 2.62, 2.12, 2.00), could be methylated and then react with CO. In the previous study, a similar complex was synthesized that had oxidation states of Ni^{II}–Ni^{0}, but reacted with CO aftermethylation at a rate that is ~37 times lower than the Ni^{II}–Ni^{I} compound. Other studies in the Hegg lab with model compounds of Ni_d indicate that Ni_d may be directly involved in the chemistry because the bisamidate ligation causes the Ni^{III}/Ni^{II} redox potential to be much lower than previously thought.[53] This finding raises the possibility that Ni_d(III) is a viable intermediate andNi_d could be considered for a role in the internal redox chemistry in the ACS mechanism.

(V) Enzymatic reactions involving CO and CO_2

Table 2 summarizes the major reactions that involve CO or CO_2 as substrate or product. The carboxylation and decarboxylation mechanisms are described in greater detail in Frey and Hegeman, 2007.[54]

Decarboxylation reactions are facilitated by the electron accepting nature of the groups next to the carboxyl leaving group and this electron accepting nature can be bestowed through cofactors such as thiamine pyrophosphate (TPP) and pyridoxal-5′-phosphate (PLP). TPP is utilized as a cofactor by *α*-ketoacid decarboxylases and oxidoreductases whereas PLP is used more often by amino acid decarboxylases. The structures of these cofactors and the mechanism of a generic TPP-catalyzed decarboxylation are depicted in Fig. 6. These decarboxylation reactions have been studied to a high degree and many of the intermediates have been identified spectrophotometrically and by crystallography.[55] Both types of cofactors and the carboxyl group eliminations that they catalyze involve intermediates where the substrates are covalently bound to the cofactor. Many of the reactions also have radical intermediates, as exemplified by PFOR,[56] which is described later in this review.

Decarbonylation is involved in various enzymatic reactions. The decarbonylation reaction of ACS is discussed in detail below. During maturation of the hydrogenase active site, the CO ligand for the H-cluster of the Fe–Fe dependent hydrogenases is derived from tyrosine.[57] During degradation of the porphyrin ring of heme, heme oxygenase releases CO, which serves as a signaling molecule for different physiological processes.[58] Other enzymes that release CO as a product are 3-hydroxy-4-oxoquinoline-2,4-dioxygenase,[59] quercetin-2,3-dioxygenase,[60] octadecanal decarbonylase[61] and acireductone dioxygenase.[62] In other reactions, CO is a substrate. CODH can oxidize CO to CO_2 and ACS uses CO as one of the three substrates to synthesize acetyl-CoA.[15]

CO_2 is also reduced to formate by formate dehydrogenase according to the following equation:

$$CO_2 + H^- \leftrightarrow HCO_2^- \quad (3)$$

There are different types of formate dehydrogenases, including molybdenum and tungsten-dependent ones, with selenocysteine, FMN, and Fe–S clusters as additional cofactors.[63,64] Some formate dehydrogenases do not have prosthetic groups.[65] Formate dehydrogenase is a metabolically important enzyme for many different organisms because it catalyzes the initial incorporation of CO_2 into cellular metabolism through reduction to formate. There is also variability in the electron acceptors used by this enzyme. Formate dehydrogenases from aerobic, anaerobic bacteria, yeast and plants can use NAD^+ or $NADP^+$ as electron acceptors. Anaerobic formate dehydrogenase complexes contain molybdenum, tungsten, selenium, Fe_4S_4 clusters, and heme *b* as cofactors and electron transport centers, and can reduce membrane bound molecules such as menaquinone, cytochromes in *E. coli* or F-420 in methanogenic bacteria.[66–69] Formate dehydrogenase from *Moorella thermoacetica* reduces

CO_2 by using electrons from NADPH. Nitrate reduction in *E.coli* is coupled to the formate dehydrogenase activity and presence of cytochromes in wild type cells.[70]

(A) CO oxidation

As mentioned earlier, some organisms are able to use CO as a source of electrons and carbon. Many other microbes are able to catalyze the oxidation of CO while growing on other carbon and energy sources. The known CO oxidizers are summarized in Table 3 and the reactions they catalyze are described in the following sections.

(1) A Mo-dependent CODH catalyzes aerobic CO oxidation and CO_2 reduction

(a) Aerobic CO oxidizing microbes: Microbial carbon monoxide oxidation was first discovered in aerobic organisms and the term *carboxidobacteria* has been coined to describe aerobic bacteria with the ability to oxidize CO. The first isolated strain was named *Oligotropha carboxidovorans*[71] to indicate that it eats everything, but devours CO. *O. carboxidovorans* has been a model organism for studies of aerobic CO oxidation. This organism consumes CO and O_2 with a stoichiometry of 2 : 1, as shown in eqn (4).[72] The diversity of currently known aerobic CO oxidizers has been reviewed.[73]

$$2\mathrm{CO}+\mathrm{O_2} \rightarrow 2\mathrm{CO_2}\ \Delta G^{\circ}=-123\,\mathrm{kcal\,mol^{-1}}\ (-514\,\mathrm{kJ\,mol^{-1}}) \quad (4)$$

(b) Metallocenters in the aerobic Mo-Cu CODH: The enzyme used for aerobic CO oxidation is a molybdenum-, copper-, iron–sulfur- and flavin-containing hydroxylase that is unrelated to the Ni-dependent CODH found in anaerobic bacteria and archaea. Aerobic CODH is a dimer of hetero-trimers consisting of CoxS, which harbors two Fe_2S_2 clusters, CoxM, which has non-covalently bound FAD, and CoxL, which contains the molybdopterin active site (Fig. 3). The amino acid sequences of the Cox subunits are most similar to those of molybdenum hydroxylases like xanthine oxidoreductase.[74] Buried in the large subunit, the Mo-pterin active site is connected to the surface of the protein by a 17 Å hydrophobic channel. The CODH subunits are arranged so that the two Fe_2S_2 clusters are between the buried Mo-pterin active site and FAD near the surface.[27] X-ray crystallographic studies of a high specific activity (23.2 U mg^{-1}) preparation of *O. carboxidovorans* CODH (94% active) showed that the active site contains the molybdopterin cytosine dinucleotide (MCD) cofactor, molybdenum, and copper (Fig. 3).[75] Evidence for this Cu included anomalous difference Fourier maps from data collected at the Se-K- and Cu-K-absorption edges, and detection by EPR of Cu removed from the enzyme upon treatment with CN^-. Furthermore, activity is proportional to both Cu and cyanolysable sulfur content.[76] The Cu atom is coordinated by the backbone nitrogen and the sulfur of Cys388, and is bridged by an inorganic sulfur atom to Mo. Molybdenum is coordinated by the MCD cofactor and two oxygen ligands, with all five ligands arranged in a distorted square pyramidal geometry. The structure of the active site has been confirmed by a subsequent crystal structures of inactive and fully constituted active CODH,[77] and by X-ray absorption spectroscopy.[76]

(c) Maturation of the active site of the Mo-Cu CODH: The complete sequence of events and set of chaperones required for active site maturation is not known. Genes encoding the three CODH subunits and presumably most of the accessory proteins needed for active site synthesis are found in the *cox* (for carbon monoxide oxidase) or *cut* gene cluster. In *O. carboxidovorans*, the *coxBCMSLDEFGHIK* gene cluster is transcribed during growth on CO, but not during growth on H_2/CO_2 or on heterotrophic substrates. Transposonmutagenesis has revealed that *coxH* and *coxI* are needed for growth on CO, but not for synthesis of fully active CODH.[87] Mutation of *coxD* leads to expression of an

inactive CODH that lacks the Cu and bridging S atoms in the active site, but could be reconstituted to produce active enzyme.[88] CoxD was found to be a membrane-bound GTPase, but has not yet been purified.[88]

Incorporation of Mo depends on its availability in the cell. Excess tungsten (W) inhibits Mo transport into cells[89] and, based on X-ray crystallographic studies of CODH from cells grown in the absence of Mo, the molybdopterin portion of the MCD cofactor is missing and only 5′-cytidine diphosphate is present.[90]

(d) Spectroscopic and Kinetic studies of the Mo-Cu CODH: Based on the Cu-K-edge EXAFS spectra, the oxidized and CO-reduced CODH show nonlinear coordination of Cu by two sulfurs,[76] which is consistent with coordination by the Mo–Cu bridging sulfur and by Cys388, as seen in the crystal structure of high-activity CODH.[75] Reduction by CO shifts the Mo-K-edge by 1.6 eV, consistent with two-electron reduction of Mo(VI) to the Mo(IV) state. In addition, reduction appears to convert one of the *oxo*-groups to a hydroxyl and to cause slight changes in the Mo–S distances.

Crystallographic studies of the oxidized, reduced and n-butylisocyanide-treated enzyme suggested a mechanism for CO oxidation.[75] The oxidized and reduced active sites have very similar geometries, with a small increase in the distance between Mo and Cu, and between Mo and its hydroxo-ligand. In the structure with bound n-butylisocyanide, the CN moiety was inserted between Cu and the metal-bridging sulfur, with C bound to sulfur and to the Mo *hydroxo*-ligand, and N coordinated to Cu, suggesting that CO similarly inserts within the Cu–S bond. It was suggested that the next step in the reaction involves electron transfer through sulfur to Mo and attack by the Mo-bound OH to form a S–CO_2 species. On the other hand, two computational studies indicate that the proposed S–CO_2 is not a catalytic intermediate, that CO would bind to Cu without the insertion between Cu and S, and that the Cu–S bond could remain intact throughout the catalytic cycle. Both studies proposed the bisoxo form of Mo (rather than Mo coordinated by *oxo* and *hydroxo* ligands) as the species needed for formation of the C–O bond.[91,92]

Two recent kinetic studies address the reductive and oxidative half reactions of *O. carboxidovorans* CODH.[106,107] The k_{cat} was determined to be 93 s^{-1} and the K_m for CO is 11 μM (at the optimal pH of 7.2). Studies of the reduction by excess CO show that CO binds rapidly, then undergoes rate-limiting oxidation that leads to reduction of the two iron–sulfur clusters at a rate constant (~90 s^{-1}) that is similar to the value of k_{cat}. The absorbance changes from FAD indicate that the two-electron reduction of FAD involves a flavin semiquinone intermediate.[106] Quinones, not cytochromes, are the likely physiological electron acceptors.[107]

(2) CO/CO_2 conversion by the Ni-CODH in anaerobic microbes

(a) Cellular roles of different Ni-CODHs: Like the aerobic enzymes, the anaerobic Ni-CODHs catalyze reaction (1). The Ni-CODH enables these organisms to grow on CO as the sole source of carbon and energy.[96,108] In the cell, different CODHs are used for CO oxidation or for CO_2 reduction. The varied functions for CODHs are exemplified in *C. hydrogenoformans*, which encodes five CODHs that have been placed into separate sub-families by phylogenetic analysis,[109] with sequence identity as low as 30% between the most distantly related pairs of sequences across these sub-families. Three of the five *C. hydrogenoformans* CODHs have been purified and characterized. CODH I and II, which share 59 percent sequence identity, are localized at the inner side of the cytoplasmic membrane, but are apparently very loosely associated with the membrane.[20] Based on reconstitution of CO-dependent H_2-evolving activity, CODH I appears to couple CO oxidation to H_2 formation by a membrane-bound hydrogenase, which is hypothesized to

generate a transmembrane H^+ gradient for ATP synthesis.[110] CODH II was hypothesized to couple CO oxidation to reduction of cellular electron carriers, based on its ability to stimulate CO-dependent $NADP^+$ reduction in cytoplasmic fractions.[20]

CODH III shares 49% and 46% sequence identity to CODH I and II, respectively, but its sequence[109] is most similar to the well-characterized CODH (*acsA*) from *M. thermoacetica*[111] that is involved in the Wood-Ljungdahl pathway and is part of the *acs* gene cluster, which also contains ACS, the CFeSP subunits and methyl transferase.[112,113] This type of CODH can reduce CO_2 to CO, which ACS utilizes for acetyl-CoA synthesis, or oxidize CO, thus donating electrons to cellular redox carriers. Homologous genes occur as an operon in methanogenic archaea.[114,115] In *M. thermoacetica*, CODH is isolated in a complex with ACS,[116,117] while, in at least some methanogens, a large acetyl-CoA decarbonylase/synthase (ACDS) complex can be purified that includes CODH, ACS, both subunits of the CFeSP and a small subunit that tightly associates with the CODH subunit.[118,119] Some methanogenic archaea can oxidize CO when they express the Wood-Ljungdahl pathway to oxidize acetate to obtain electrons for methanogenesis.[120–123]

CODH IV and CODH V from *C. hydrogenoformans* have not been purified, and their cellular roles have not been defined. Based on surrounding genes, CODH IV is hypothesized to play a role in responding to oxidative stress. The sequence of CODH V differs most from the other CODH sequences, and its gene neighborhood does not indicate its physiological role.[109]

(b) CO sensing mechanisms in microbes, CooA & RcoM: Some microbes contain a CO sensor that activates transcription of genes involved in CO metabolism. The CO-sensor that has been studied and understood the most is CooA from *Rhodospirillum rubrum.*[124] CooA is a heme-binding protein. When CO binds to the heme cofactor, it causes a conformational change that leads to DNA binding.[125] Some homologues of CooA are present in other organisms, such as the transcriptional activator, CRP of *E. coli*, even though they respond to different effectors and have different physiological roles. There are also more closely related homologs in organisms that are either known to or expected to utilize CO, but none of them have been as biochemically well-characterized as CooA. The bacteria in which the CooA analogs were found were *Azotobacter vinelandii, Carboxydothermus hydrogenoformans* strains, and *Desulfuvibrio* species.[126] CooA not only senses CO, but it is also a sensor of redox potential, since it is reduced below −300 mV and can only bind CO in the reduced form. There is a ligand switch between the oxidized (Cys ligand) and reduced (His ligand) forms of the enzyme while CO replaces the other axial ligand, Pro.[124]

Another CO responsive transcriptional regulatory protein called RcoM has been idenified in various facultative aerobic microbes.[127] Like CooA, RcoM binds heme; however, the heme binds to a PAS instead of a CRP-like domain.

(c) Metal-centered cofactors of the Ni-CODH: Over the last decade, several CODHs have been crystallized, including the *R. rubrum* CO-induced CODH,[128] CODH II from *C. hydrogenoformans*,[129] the CODH/ACS complex from *M. thermoacetica*[44,130] (Fig. 4) and the CODH component of the ACDS complex of *Methanosarcina barkeri*.[131] The structures of the *M. thermoacetica* CODH overlay with those of the CODHs from *R. rubrum* and *C. hydrogenoformans* with root mean square deviations of 1.0 and 0.8 Å, respectively.[44] All of the bacterial CODHs crystallize as homodimers in which each subunit contains the unique $NiFe_4S_4$ active site (the C-cluster), an Fe_4S_4 B-cluster, and an additional Fe_4S_4 cluster, the D-cluster, which bridges the two subunits. An N-terminal helical domain ligates the B- and D-clusters and two (a central and a C-terminal) α/β Rossmann domains provide the ligands for the C-cluster. The Rossmann domains overlay with a root mean square deviation of 1.7

Å.[129] The *M. barkeri* CODH contains the three domains found in the bacterial CODHs along with very similar B-, C- and D-clusters, but in addition, has another domain that ligates two additional Fe_4S_4 clusters, and an ε-subunit, which is not found in bacterial CODHs and has an unknown function.[131]

(d) Structure and Maturation of the active site C-cluster of the Ni-CODH: The basic composition of the C-cluster (Fig. 4), which has been seen in X-ray crystal structures of CODH I, II and III from different organisms, is a Fe_3S_4 cluster, ligated by three cysteine residues, and connected to a binuclear NiFe site. Exhibiting approximately planar or distorted tetrahedral coordination, the Ni is bridged to two sulfurs of the Fe_3S_4 moiety and coordinated by a fourth cysteine. The Fe of the NiFe site is called ferrous component II (FC II) and is ligated by a histidine and a fifth cysteine ligand that forms a μ_3-S coordination at one corner of the cubane. In the first structure of the *C. hydrogenoformans* CODH II[129] an additional inorganic S was modeled as a bridge between Ni and FC II. The importance of the μ_2-S bridging Ni and Fe is not clear, although in a recent crystal structure of CO_2,[132] water, and cyanide[133]-bound CODH, the bridging sulfur is not present, and instead CO_2 and cyanide are bound to Ni and water/hydroxide are bound to Fe.[132] In the *R. rubrum* CODH structure,[128] a Cys residue (Cys 531 in Fig. 4c) bridges Ni and FC II, while in the *M. thermoacetica* CODH/ACS structure,[130] this cysteine is modeled in different positions, depending on whether it coordinates Ni or FC II. These last two structures also have a small molecule, modeled as CO, in the apical coordination site of Ni.

The CODH/ACS gene cluster in bacteria contains two small genes, *cooC* and *acsF*, that are hypothesized to play a role in active site maturation. In *R. rubrum*, which encodes only monofunctional CODH, *cooC* is found in a *cooCTJ* gene cluster. Deletion of portions of this gene cluster increases the concentration of Ni needed for CO-dependent growth.[134] CooC has been purified from *R. rubrum*. It has a nucleotide-binding domain, which supports ATPase and GTPase activities. Cell-extract experiments with wild-type and deletion strains showed that insertion of Ni into Ni-deficient CODH from *R. rubrum* could be enhanced, in an ATP dependent fashion, by CooC.[135]

(e) Bimetallic Ni-CODH mechanism: Early studies on CODH from *Rhodospirillum rubrum* showed that Ni and FeS clusters are both involved in CO oxidation.[136,137] Spectroscopic studies demonstrate that the C-cluster can equilibrate among at least three different oxidation states: C_{ox}, which is EPR-silent and C_{red1} ($g_{x,y,z}$ = 2.01, 1.81 and 1.65, g_{av} = 1.82) and C_{red2} ($g_{x,y,z}$ = 1.97, 1.87 and 1.75, g_{av} = 1.86), which are EPR active. In *M. thermoacetica* CODH, C_{red1} is formed by one-electron reduction of C_{ox}, with a midpoint potential of −220 mV, and C_{red2} is formed upon lowering the redox potential to around −530 mV.[138] When CODH is treated with CO, C_{red1} is rapidly converted into C_{red2}; then the g = 1.94-type EPR spectrum ($g_{x,y,z}$=2.04, 1.94, 1.90) of the B-cluster is observed.[139] Similar changes occur when CODH is reduced by dithionite or Ti(III)citrate with formation of the C_{red2} EPR signal from the C-cluster and the g=1.94 spectrum of the B-cluster.[138]

As described in Fig. 7, CODH uses a ping-pong mechanism.[116,140] In the first half-reaction, CO reduces CODH, forming CO_2 and, in the second half-reaction, an electron acceptor binds and reoxidizes CODH. Even with the *M. thermoacetica* enzyme that has low activity relative to the *C. hydrogenoformans* enzyme, the reaction with CO occurs so quickly that the temperature needed to be lowered to 5 °C to follow the freeze quench EPR and stopped flow experiments. The first observable changes occur on the C-cluster as C_{red1} is converted to C_{red2} with a rate constant of 400 s^{-1} (equivalent to 12 000 s^{-1} at the optimal growth temperature of 55 °C), yielding a bimolecular rate constant of 4.4×10^6 M^{-1} s^{-1} at 5 °C (1.4×10^8 M^{-1} s^{-1} at 55 °C). Next, the B-clusters are reduced with a rate constant of 60 s^{-1} (at 5 °C and 180 μM CO). The k_{cat} for CO oxidation at 5 °C is 47 s^{-1} by the *M. thermoacetica*

CODH,[139] while it is 600 s^{-1} at 55 °C and pH 7.6.[140] The spectroscopic properties of the C-cluster and CO oxidation rate are pH dependent. The g_{av} = 1.82 EPR spectrum of the C_{red1} form of $CODH_{Mt}$ shows pH-dependent broadening, with an inflection point at pH 7.2. Both k_{cat} and $k_{cat}/K_{m(CO)}$ are pH dependent, with pK_a values at 7.7 for k_{cat}/K_m and at 7.0 and 9.5 for k_{cat}.[140]

CO oxidation appears to occur at the NiFe subcomponent of the C-cluster *via* a bimetallic mechanism as described in Fig. 7. *Step 1* involves binding of CO to the Ni site of the C-cluster, as suggested by X-ray crystallographic studies of CO bound to a methanogenic CODH[131] and by Fourier transform infrared (FTIR),[142] X-ray absorption[143] and X-ray-crystallographic[133,144] studies of the complex of CODH with CN^-, a competitive inhibitor with respect to CO.[145] Two modes of CO and CN^- binding have been observed: one with an acute Ni–C–N/O angle[131,133] and another that is linear.[144] The existence of two Ni–CN conformations is consistent with the observations of CN^- as a slow binding inhibitor[143,145,146] and of two M-CN vibrations in the IR spectrum (at 2078 cm^{-1} and 2037 cm^{-1}),[147] with the former peak at the expected position for a linear Ni–C–N complex and the latter for a bent complex. *Step 2* involves the deprotonation of bound water. His and Lys residues are involved in proton transfer during catalysis.[148] The metal–OH_2 complex should have a fairly low pK_a, as in carbonic anhydrase,[149] facilitating formation of an active hydroxide. Deprotonation of water may also involve base catalysis by Lys or His residues near the C-cluster,[128,129] a proposal supported by mutagenesis experiments.[148] In *Step 3*, OH^- from the Fe-hydroxide attacks Ni–CO to form a carboxylate that bridges the Ni and Fe atoms.[132] In *Step 4*, elimination of CO_2 is coupled to two-electron reduction of the C-cluster (Ni“0”) and the binding of water. The two-electron reduction could generate a true Ni^0 state[150] or, more likely, a state in which the electrons delocalize into the Fe and S components of the C-cluster. Freeze quench EPR studies show that when the resting state of CODH (C_{red1}) reacts with CO, it converts rapidly (1.4×10^8 M^{-1} s^{-1}) to another distinct paramagnetic state called C_{red2}, before electrons are transferred to the B- and D-clusters.[139,151] Finally, in *Step 5* electrons are transferred from the reduced B- and D-clusters to an external redox mediator, *e.g.*, ferredoxin. At high CO concentrations, Step 5 becomes rate limiting.[139,151] Each of the steps above can occur in reverse to catalyze the reduction of CO_2.

(f) Electrochemical studies of the Ni-CODH: CODH can catalyze CO_2 reduction with little to no overpotential. When CODH was directly attached to a glassy carbon working electrode and cyclic voltammetry was performed in the presence of CO_2 and methyl viologen, CO was formed at a rate that is half maximal at a redox potential of −0.57 V at pH 6.3, which was very close to the theoretical potential of the CO_2 reduction at this pH (−0.48 V).[152] Similarly, the midpoint potential for the one-electron reductive activation of the *R. rubrum* CODH (adsorbed to a pyrolytic graphite electrode) is −418 mV.[153] When the *C. hyrogenoformans* Ni-CODH I was adsorbed on a pyrolytic graphite edge (PGE) electrode in an anaerobic cell, it was active in both directions with the electrocatalytic reaction being dependent on both the pH and CO/CO_2 concentrations.[154] At low pH values, the rate of CO_2 reduction surprisingly exceeds that of CO oxidation.[154] The high catalytic efficiency of CO_2 reduction at the thermo-dynamic potential for the CO_2/CO couple appears to be due to its ability to undergo rapid successive two-electron transfers coupled to proton transfer,[154] unlike nonenzymatic catalysts that reduce CO_2 through a high-energy $^{\bullet-}CO_2$ anion radical.[155] Electrochemical studies also revealed two reversible processes with activation/inactivation potentials of −50 mV and −250 mV.[154]

CODH can be coupled to other electrochemical reactions. For example, when CODH was adsorbed on graphite platelets along with *E. coli* hydrogenase, H_2 was produced, coupling CO oxidation to proton reduction.[156] This is analogous to the industrial water gas-shift

reaction (eqn (2)). CODH could also be coadsorbed with an inorganic ruthenium complex onto TiO_2 nanoparticles, allowing the photoreduction of CO_2 to CO using very mild reductants.[157]

(3) Metal centers involved in energy conservation by CO-utilizing bacteria

(a) Metallocenters involved in energy conservation coupled to CO oxidation in aerobic microbes: Aerobic bacteria oxidize CO using O_2 as a final electron acceptor, according to the overall reaction shown in eqn (4). The respiratory chain used during aerobic growth on CO involves direct reduction of the quinone pool by the FAD bound to CODH,[107] which would pass electrons to the membrane-bound electron transport chain, including cytochromes.[107] It is interesting that growth and respiration of most aerobic bacteria (including carboxidovores!), are inhibited by CO, because CO binds to and inhibits the cytochromes of the terminal oxidase of the respiratory chain. To circumvent CO poisoning of their respiratory chains, carboxidotrophic bacteria, including *Pseudomonas*, *Alcaligenes*, and *Arthrobacter*, have evolved a CO-insensitive terminal oxidase that contains cytochrome *o* (cytochrome b_{653}) that does not bind CO.[158] Thus, at least in *P. carboxidovorans*, a CO-sensitive cytochrome *a*-containing cytochrome *c* oxidase is used during oxidation of heterotrophic substrates, while the CO-insensitive cytochrome *o*-containing cytochrome *c* oxidase is used during oxidation of CO or H_2.[159,160] Thus, the energy conserving electron transfer chain would involve CODH, the quinone, cytochrome *c*, and the cytochrome *o*-containing terminal oxidase. Proton translocation that would be coupled to ATP synthesis presumably occurs with the oxidase that links the quinone to cytochrome *c* and the terminal oxidase. Similar branched respiratory chains have been found in many H_2-oxidizing proteobacteria.[161]

(b) Metallocenters involved in energy conservation by anaerobic growth on CO: Some anaerobic microbes like acetogens are able to use the Wood-Ljungdahl pathway for energy conservation as well as carbon assimilation during autotrophic growth on H_2/CO_2 or CO.[96] *M. thermoacetica* has phospho-transacetylase[162] and acetate kinase, which convert acetyl-CoA to acetate and ATP by substrate-level phosphorylation. However, ligation of formate to tetrahydrofolate in the methyl branch of the pathway requires ATP,[163] so there is no net synthesis of ATP by substrate-level phosphorylation by the Wood-Ljungdahl pathway. Therefore, acetogens growing autotrophically by this pathway must synthesize ATP by gradient-driven ATP synthases.

The oxidation of CO in *M. thermoautotrophica* is coupled to reduction of the *b*-type cytochromes present in the membranes in a process that involves methylenetetrahydrofolate reductase.[164] The following electron transport chain has been proposed: oxidation of CO coupled to reduction of cytochrome b_{559}, which then reduces methylenetetrahydrofolate or menaquinone and cytochrome b_{554}, which would finally reduce rubredoxin.[165] However, the step that extrudes protons in the proposed electron transport chain is still not known. The free energy change of reduction of methylene-tetrahydrofolate to methyl-tetrahydrofolate ($\Delta G_0' = -57.3$ kJ mol^{-1}) would be sufficient for ATP synthesis.[166] A proton-pumping F_1F_0 ATPase is found in *M. thermoacetica*.[167,168] *M. thermoacetica* membrane vesicles prepared by gentle lysis of cells, which does not disrupt the association of CODH with the membrane, can generate a proton motive force when exposed to CO.[169]

While some acetogens like *M. thermoacetica* seem to use a cytochrome-based proton-coupled electron transfer pathway, others, like *Acetobacterium woodii* contain membrane-bound corrinoids instead of cytochromes that have been suggested, in analogy to the corrinoid-containing, Na^+-pumping methyltetrahydro-methanopterin: coenzyme M methyltransferases of methanogenic archaea, to be involved in energy conservation.[170,171]

Experiments with resting cells of *A. woodii* have shown that the methylenetetrahydrofolate reductase requires sodium, and is probably the electron-accepting step for Wood-Ljungdahl pathway-linked respiration.[172] Na^+ is taken up into inverted membrane vesicles, which is coupled to acetogenesis.[173] The Na^+ dependent ATPase was purified and shown to be an unusual F_1F_0 ATPase,[174] with two types of rotor subunits, *e.g.*, two bacterial F(0)-like c subunits and an 18 kDa eukaryal V(0)-like c subunit.[175,176] Acetate formation and autotrophic growth by *A. woodii* require sodium.[172] Given the phylogenetic diversity of acetogens, there may be many different mechanisms for coupling oxidation of other substrates to ATP synthesis during acetogenic growth and many different proton or sodium-translocating enzymes. One mechanism that has been recently shown is coupling of H_2 oxidation and caffeate reduction to ATP synthesis in *A. woodii* by an Rnf-type NADH dehydrogenase complex that accepts electrons from ferredoxin and reduces NAD^+ (NADH is the electron donor for caffeate reduction), while translocating Na^+.[177,178] Sodium transport in this systemis supplemented by a sodium translocating pyrophosphatase that uses PPi generated when ATP is cleaved to activate caffeate.[179] Whether these Na^+ translocating systems are also coupled to the Wood-Ljungdahl pathway is not yet known. A second route for energy conservation during anaerobic growth on CO is coupling CO oxidation and proton reduction to H_2 by separate enzymes to ATP formation as described above for *C. hydrogenoformans* CODH I.

(B) PFOR and the production and utilization of CO_2

PFOR catalyzes the oxidative decarboxylation of pyruvate to form acetyl-CoA, CO_2 and two reducing equivalents, which are transferred to ferredoxin:

$$\mathrm{Pyruvate + CoASH \rightarrow Acetyl-CoA + CO_2 + 2H^+ + 2e^-} \quad (5)$$

PFOR also catalyzes the thermodynamically uphill reverse reaction to generate pyruvate,[180,181] which enters the reductive TCA cycle[182,183] to generate intermediates for cell carbon synthesis. Found in archaea, bacteria, and anaerobic protozoa,[184] PFOR is the target for nitroimidazole drugs, *e.g.* metronidazole and tinidazole, which target various infectious anaerobic microbes, including *Clostridium difficile* (diarrhea) and *Helicobacter pylori* (ulcers).[185,186]

PFOR and other oxoacid oxidoreductases can be homodimeric, heterodimeric or heterotetrameric[187] and appear to have evolved by rearrangements and fusions of four ancestral genes.[188,189] The *Desulfovibrio africanus* PFOR, whose structure is known,[190] is homodimeric like the highly homologous *M. thermoacetica* protein, the fusion product of all four genes. As shown in Fig. 8, PFOR contains thiamine pyrophosphate (TPP) and three Fe_4S_4 clusters per monomeric unit, with TPP and Cluster A being deeply buried within the protein and the other two clusters (B and C), which are in a ferredoxin-like domain, leading to the surface, where interactions with a redox partner such as ferredoxin can occur. Clusters A–B and B–C are separated by ~13 Å (center-to-center) and exhibit midpoint redox potentials of −540, −515, and −390 mV.[191]

The PFOR mechanism (Fig. 9) has been studied by transient and steady-state kinetic studies.[192] Carbon 2 of the thiazolium ring of TPP undergoes deprotonation to generate an ylide, which catalyzes nucleophilic attack on the C2 atom of pyruvate, generating a lactoyl-TPP adduct that undergoes decarboxylation to generate a 2α-hydroxyethylidene-TPP (HE-TPP) intermediate. HE-TPP is a highly reactive carbanion (“active aldehyde”) that undergoes a one-electron transfer from Cluster A to Cluster B, thus generating a HE-TPP radical intermediate. The HE-TPP radical, recently assigned incorrectly as a sigma radical based on X-ray crystallographic studies,[193] has been shown to be a pi-type radical benefiting

from stabilization among at least 7 different resonance forms, with the unpaired spin delocalized among the atoms of the HE group and the thiazole ring.[194] The HE-TPP radical then transfers one electron to an internal Fe_4S_4 cluster in a reaction that binding of CoA enhances by 10^5-fold,[192,195] with the *thiol* group of CoA *alone* lowering the barrier for electron transfer by 40.5 kJ/mol.[192] Finally, the reduced enzyme transfers two electrons to ferredoxin.

Pyruvate oxidase appears to follow a mechanism similar to that of PFOR, with phosphate taking the place of CoA and molecular oxygen replacing ferredoxin as electron acceptor. This enzyme contains TPP, FAD, Mg^{2+} and Mn^{2+} and generates acetyl-Pi and H_2O_2 as products.[55,196,197]

(C) The CFeSP and methyltransferase (MeTr)

MeTr (AcsE)[162] catalyzes transfer of the methyl group of CH_3–H_4folate to the Co(I) center in the CFeSP (AcsCD)[198,199] to form the first organometallic intermediate in the Wood-Ljungdahl pathway, CH_3–Co(III) (Fig. 2). In this reaction, the CFeSP acts as the methyl acceptor and methyl-H_4folate acts as the methyl donor. The reaction takes place *via* an S_N2 mechanism in which the cob(I)amide state of the CFeSP engages in a nucleophilic attack on the methyl group of methyl-H_4folate, forming the methylcob(III)amide state of the CFeSP and releasing H_4folate.[200] This reaction appears to occur *via* the following steps, as shown in Fig. 10. First, there is a pH-dependent conformational change in the protein.[201] MeTr then binds methyl-H_4folate and the CFeSP in a random mechanism.[202] At this point, methyl-H_4folate is protonated from solvent at the N5 position (where the methyl group is bound) through an extended H-bonding network that involves an Asn residue that interacts with N5.[203] This protonation places a positive charge at N5, activating the methyl group and making the methyl donor more electrophilic.[200,204] The methyl group is then transferred to CFeSP. MeTr, H_4folate, and the methylated CFeSP rapidly dissociate after methyl transfer occurs, ending the first phase of the CFeSP-catalyzed reaction.[204]

After dissociation from the ternary complex formed in the first methyl transfer reaction, the methylated CFeSP serves as the methyl donor to ACS[205] in a reaction that is described in more detail below. Briefly, the Ni center of the A-cluster of ACS engages in an S_N2 attack on the methylcob(III)amide, which methylates ACS and regenerates Co(I) for the next round of catalysis by MeTr.[206] Then, the methyl-Ni form of ACS undergoes a carbonyl insertion to produce an acetyl-Ni intermediate that undergoes nucleophilic attack by CoA to generate acetyl-CoA.[207]

(D) CO as a metabolic intermediate during growth on CO_2

When acetogens grow on pyruvate, CO is formed as a metabolic intermediate that is generated by the combined actions of PFOR, which catalyzes the oxidative decarboxylation of pyruvate, and CODH, which reduces the CO_2 to CO.[208] Carbon monoxide has also been shown to be produced during growth of aceticlastic methanogens.[209] The CO that is generated, however, is sequestered within a channel in the CODH/ACS complex as revealed by enzymatic studies[210,211] and by X-ray crystallography.[44,212,213] When CODH/ACS crystals were subjected to high pressures of Xenon gas, Xe atoms were located at 19 discrete sites in the protein, allowing one to map out a path for the CO molecules between the active sites.[212] Mutations of residues to block the movement of CO in the channel led to enzymes with much lower CODH and ACS activities.[214] A similar gas channel was observed in the crystal structure of the acetyl-CoA decarbonylase/synthase complex of aceticlastic methanogens.[215] The presence of a CO channel underlines the problem of the low availability of CO in the environment and the need to sequester the produced CO and not lose it to irrelevant reactions or to diffusion out of the cell.

(E) The synthesis of acetyl-CoA by ACS

(1) The structure of ACS—ACS is a nickel protein that is involved in the final step of acetyl-CoA synthesis from CO generated by CODH, the methyl group donated by the CFeSP, and CoA. ACS consists of three domains.[15,141,216,217] The N-terminal Rossmann-fold domain interacts with the CODH subunit and contains part of the CO channel, described just above. The next two domains have novel α/β folds, and the C-terminal domain contains the A-cluster. In addition, there is an interdomain cavity rich in Arg residues that is proposed to be the binding site for CoA. During catalysis, the three domains appear to undergo large conformational changes relative to each other to accommodate the three substrates with very different sizes and coming from different directions to the active site. For example, to transfer a 15 Da methyl group from the 88 kDa CFeSP to the A-cluster makes it imperative that the ACS subunit open up to bring the A cluster and Co(III)-CH_3 of the CFeSP within bonding distance.

(2) Structure of the A-cluster—When CODH/ACS was first analyzed by EPR, the CO-treated reduced enzyme was found to exhibit a characteristic EPR spectrum with *g*-values at 2.074 and 2.028.[218] When ^{13}CO was used and when the enzyme was labeled with ^{61}Ni and ^{57}Fe, hyperfine splittings were observed, indicating that CO binds to a Ni-FeS cluster containing more than two iron atoms and that there is extensive delocalization of the unpaired electron spin among these components of the cluster; therefore, this signal was named the NiFeC signal.[218–220] Subsequently, it was found that this signal derives from the A-cluster in ACS, which consists of a Fe_4S_4 cluster that is cysteine-bridged to a dinuclear Ni center (Fig. 4d). Cys506, Cys518 and Cys528 (numbering based on *M. thermoacetica*) ligate to the iron sites in the Fe_4S_4 cluster and Cys509 bridges the Fe_4S_4 cluster and the Ni that is proximal to the Fe_4S_4 (Ni_p). Ni_p is ligated by two other Cys residues, Cys595 and Cys597, which bridges Ni_p to the distal nickel (Ni_d). The other Ni_d ligands are the backbone amide groups of Cys595 and Gly596, forming a square planar coordination and a stable +2 oxidation state for Ni_d.[44]

Initially, the metal in the proximal position was thought to be Cu because Cu was present at high occupancy in the first crystal structure (with Ni in the distal site); furthermore, activity appeared to be correlated to Cu content.[221] However, it later became apparent that a reconstituted Ni–Ni form of the A-cluster was active, while a Cu–Cu form was not.[222] Metal reconstitution experiments (using Cu^{2+} and Ni) with the acetogenic enzyme also indicated that the Cu–Ni form of ACS is inactive and the Ni–Ni form is active.[223] When methods were developed to examine activity over a wide range of Ni, Cu and Zn concentrations, it became clear that Cu and Zn readily substitute into the Ni_p site, and that the Ni–Ni enzyme is the active form of the enzyme.[224] The monomeric ACS from *C. hydrogenoformans* also contains two Ni atoms, and the activity of the enzyme correlates well with the nickel content of the monomer.[225]

X-Ray crystallographic and biochemical studies revealed that the coordination chemistry and/or the metal in the proximal site can affect the conformation of the protein, *i.e.*, the Ni–Ni form of ACS has an open conformation whereas Zn–Ni has a closed conformation.[213,226] The different conformations observed with different metals indicate a high degree of plasticity at the M_p site, which would help promote alternative coordination and oxidation ($Ni^{1+,2+,3+}$) states as ACS performs a catalytic cycle, *e.g.*, having a closed conformation to react with CO and an open conformation to react with the methylated corrinoid protein.

It is not known if chaperone proteins are involved in metal incorporation or maturation of the A-cluster. It was proposed that AcsF, encoded by one of the genes of the *acs* gene cluster, is involved in the insertion of Ni into the active site.[227]

(3) Assays and Proposed mechanisms for acetyl-CoA synthesis—the diamagnetic and paramagnetic mechanisms—In describing the mechanism of ACS, there are three major controversial and interrelated issues: (i) whether the catalytic cycle occurs through diamagnetic or paramagnetic intermediates, (ii) whether the active state of the A-cluster is a Ni^0, Ni^{1+}, or Ni^{2+} species or a spin-coupled center in which Ni^{1+} is coupled to a Fe_4S_4 cluster, and (iii) whether the first step in acetyl-CoA synthesis is carbonylation or methylation. Different views on these issues were addressed in a series of reviews.[217,228–230] Whatever mechanism is proposed, it must not conflict with the following experimental results: (i) Isotope chase experiments indicate that CO and the methyl group bind randomly to ACS to form an acetyl-ACS intermediate that reacts with CoA to form acetyl-CoA.[231] Thus, methyl-ACS and ACS-CO are both viable intermediates in the pathway of acetyl-CoA synthesis. This is consistent with experiments indicating that methylated[205,232] and carbonylated[233] forms of ACS are intermediates. (ii) The activation of ACS involves an n =1 process with an activation potential near −500 mV. Controlled potential enzymology studies measure midpoint potentials of −490 mV for the CoA/acetyl-CoA exchange[234,235] and −510 mV for the CO/acetyl-CoA exchange.[236] (iii) Transfer of the methyl group to CODH/ACS occurs by an S_N2 pathway[206] and the methyl-ACS product does not appear to exhibit an $S=\frac{1}{2}$ EPR signal.[229] (iv) The methyl group of chiral CH_3–H_4folate is converted to acetyl-CoA with retention of configuration.[237]

The competing “paramagnetic” and “diamagnetic” mechanisms differ in whether the pathway of anaerobic acetyl-CoA synthesis occurs through paramagnetic or diamagnetic intermediates.[86,231,238,239] In the Paramagnetic mechanism, shown in Fig. 11, *Step 1* involves reductive activation of Ni_p^{2+} to the active Ni^{1+} state, which can bind CO (“a” branch in red) or the methyl group (“b” branch in blue).[207] In *step 2a*, Ni_p^{1+} binds CO to form a paramagnetic Ni_p^{1+}–CO intermediate. This step can be reversed by photolysis of Ni_p^{1+}–CO, generating Ni_p^{1+}, which recombines with CO with an extremely low (1 kJ mol^{-1}) activation energy. The CO used in this step is generated *in situ* by CODH and channeled to the active site of ACS. In *step 3a*, ACS binds the methyl group to form acetyl-Ni^{3+}, which is proposed to be rapidly reduced (*step 4a*) by an internal redox shuttle to form acetyl-Ni^{2+}. Finally, in *step 5a*, CoA reacts with acetyl-ACS to release acetyl-CoA in a reaction that leads to transfer of one electron to the A-cluster to regenerate the Ni^{1+} starting species and the other to the electron shuttle, which can reduce acetyl-Ni^{3+} in the next catalytic cycle. In the lower “b” branch, reductive activation is coupled to methylation (*step 2b*), then reduction (*3b*) to generate methyl-Ni^{2+}. Then, CO binds to form the acetyl-ACS intermediate (4b), which reacts with CoA (5b), as in the “a” branch.

The diamagnetic mechanism[229] can be related to the lower path (b) except that it includes two-electron reductive activation to generate Ni[229,240] or a spin-coupled species with Ni and the cluster in the 1+ states,[239,241] methylation to generate methyl-Ni^{2+}, carbonylation to generate acetyl-Ni^{2+}, and nucleophilic attack by CoA to regenerate the active Ni“^{0}” state. The diamagnetic mechanism considers Ni^{1+}–CO to be an inhibited state and lacks the need for an internal electron shuttle. Both the paramagnetic and diamagnetic mechanisms satisfy the stereochemical requirements because they involve two successive nucleophilic attacks, *i.e.*, by Co(I) on methyl-H_4folate and by Ni(I) on the methylated CFeSP, which would lead to net retention of configuration.

The binding site for CoA on ACS is not known. Phenylglyoxal, methylglyoxal, and butanedione, which modify arginine residues, are inhibitors of ACS activity; thus an arginine residue appears to be involved in binding of CoA.[242] These modifying agents worked in the presence of CO, so CO binding does not block the modification sites. A tryptophan residue has also been implicated in CoA binding; *N*-bromosuccinamide (NBS) modifies tryptophan residues in CODH/ACS and inhibits ACS activities, and CoA binding

protects against this modification and against inhibition of activity by NBS.[243] Purification and sequencing of a peptide protected from DNPS-Cl modification by CoA identified Trp418 of the *M. thermoacetica* ACS as the tryptophan residue most likely involved in CoA binding.[244] Trp418 is part of the middle domain of ACS, and faces into a cleft in the center of the protein. Its side chain is about 24 Å from the proximal Ni in the active site, which is contained in the C-terminal domain of the protein. The ATP moiety of CoA may bind to the central domain of ACS, with the pantotheine part of the molecule stretching across the cleft in ACS so that sulfur is positioned near the active site.

(4) Intermediates trapped during the reaction, and their relationship to the two proposed mechanisms—We favor the paramagnetic mechanism. This choice is based on the results of a combination of electrochemical, isotope chase, and transient kinetic experiments. As described above and shown in Fig. 11, either CO or the methyl group can bind to ACS in the first step in acetyl-CoA synthesis. Based on stopped flow IR and freeze quench EPR studies, the only ACS-CO species that forms at catalytically relevant rates is the paramagnetic Ni^{1+}–CO species.[233] Ironically, this species was identified by EPR spectroscopy[218,219] long before it was even known that CODH and ACS have different active sites. Other transient kinetic studies following formation and decay of the EPR-active Ni^{1+}–CO species also have established its catalytic competence as an intermediate in acetyl-CoA synthesis.[245–247] Furthermore, the midpoint potential for formation of the NiFeC species (−540 mV)[246] is consistent with the values for reductive activation of ACS in the CO/acetyl-CoA[236] and CoA/acetyl-CoA exchange reactions.[235]

Some favor the diamagnetic mechanism of acetyl-CoA synthesis. Because acetyl-CoA synthesis is inhibited at high CO concentrations, it was suggested that the Ni(I)–CO species might be a reversible, off-pathway species and not an intermediate. [248] However, at non-inhibitory CO concentrations (100 μM), acetyl-CoA synthesis and formation of the Ni(I)–CO species take place at similar turnover numbers (1 s^{-1}) while decay of the species occurs much faster (6 s^{1-}), suggesting that this species is indeed a catalytically competent intermediate.[245] The other apparent inconsistency with the paramagnetic mechanism is that the reaction of reduced ACS with the methylated CFeSP generates Co^{1+} and an EPR-silent product on ACS, indicating it is a CH_3–Ni^{2+} species. The paramagnetic mechanism would predict the initial product of this S_N2 reaction would be CH_3–Ni^{3+}. Lindahl also showed that ACS can be methylated, purified and stepped through the rest of the reaction without any external reactants or reductants other than CO and CoA (which donates two electrons).[249] The methyl-ACS state was also shown to react with the CFeSP to regenerate methyl-Co^{3+} or with CO and CoA to make acetyl-CoA.[205] Thus, if acetyl-CoA synthesis occurs according to the paramagnetic mechanism as shown in Fig. 11, an internal one-electron transfer would be required to reduce CH_3–Ni^{3+} to a more stable CH_3–Ni^{2+} state. Evidence was recently presented for this “one-electron shuttle”.[236] It was shown that the shuttle can transfer an electron to ferredoxin, allowing the quantification of the number of electrons in each of the intermediate states of ACS. However, it has not yet been determined where on ACS this shuttle resides.

As shown in Fig. 11, CO or the methyl group are proposed to bind to a Ni^{1+} species to generate a Ni^{1+}–CO or methyl-Ni^{3+} species, respectively. Recent studies indicate that this is an unstable intermediate that is transiently formed in a reaction that is kinetically coupled to CO binding. When the Ni(I)–CO state was photolyzed at low temperatures (<30 K), a new EPR signal was observed, which was attributed to the formation of an unstable Ni(I) state in which the CO had dissociated.[207] This Ni^{1+} species has an exceptionally low activation energy for recombination of CO to reform the Ni(I)–CO species. This low activation energy could reflect the recombination of CO from the hydrophobic pocket (an alcove) near Ni_p observed in the crystal structure.[212]

Conclusions

Redox-active metal centers are at the catalytic center and the electron-transfer sites of many one-carbon reduction reactions. Over the past decade, there have been many significant findings related to the metabolism of CO_2 and CO, which impact our understanding of the biogeochemistry and the evolution of life on Earth. Three novel CO_2 fixation pathways have recently been discovered. Structures of many of the key enzymes involved in anaerobic CO and CO_2 metabolism have been determined and, with these structures, atomic level descriptions of radicals and metal-centered redox cofactors have been revealed. These include novel molybdenum/copper and nickel–iron–sulfur clusters as well as multiple redox centers that transfer electrons to the catalytic centers. Incisive spectroscopic and kinetic studies have trapped and characterized intermediates bound to these metal centers. Large conformational changes have been shown to move catalytic centers among various binding partners, promoting the transfer of one-carbon units. Channels within proteins have been discovered that facilitate the movement of the reactive high-energy gas CO within a protein complex. Genetic systems have become available that will open the door for site-directed mutagenesis and metabolic studies. Macromolecular complexes that are responsible for energy conservation have been identified.

Although there has been significant progress over the last decade, much remains to be learned. The novel structures provide an architectural framework for designing experiments and testing mechanistic hypotheses using a wide array of biochemical, biophysical and computational methods. It is anticipated that, by combining rapid mixing, spectroscopic and structural methods, each of the intermediates in the major CO and CO_2 fixation pathways will be captured and characterized. By reaching the intellectual goals of learning how nature catalyzes these remarkable reactions, scientists and engineers can use these natural design principles to develop catalysts that can more efficiently generate needed chemicals and fuels from simple abundant compounds like the greenhouse gas, CO_2. For example, while current nonbiological catalysts are rather nonselective and/or inefficient and require significant overpotentials (hundreds of mV) to drive the reaction, enzymes are fast (~30 000 s^{-1}) and operate without an overpotential at the thermodynamic redox equilibrium.

Because anaerobes cannot harvest as much energy from substrate oxidation as aerobes, their growth is often limited by how much energy they can generate from substrate oxidation; therefore, they have become masters at metabolic engineering. It is expected that, as a better understanding of how these organisms perform their wide array of metabolic reactions and conserve energy for growth and movement, anaerobes will become more widely used in biotechnological applications, especially as the genetic systems become more broadly applied. Thus, one can imagine microbial and biomimetic catalytic systems being key platforms for transforming simple abundant compounds like CO_2 into various fuels and chemicals that are much desired in our society.

Abbreviations

ACDS	acetyl-CoA decarbonylase/synthase
ACS	acetyl-CoA synthase
ATP	adenosine triphosphate
CBB cycle	Calvin-Benson-Bassham cycle
CFeSP	corrinoid iron–sulfur protein
CH_3-H_4 Folate	methyl-tetrahydrofolate

CODH	carbon monoxide dehydrogenase
DFT	density functional theory
EPR	electron paramagnetic resonance
FAD	flavin mononucleotide
FMN	flavin mononucleotide
MeTr	methyltransferase
MCD	molybdopterin cytosine dinucleotide
NAD	nicotinamide adenine dinucleotide
PEP	phosphoenol pyruvate
PFOR	pyruvate:ferredoxin oxidoreductase
PLP	pyridoxal-5′-phosphate
RubisCO	ribulose-1,5-bisphosphate carboxylase/oxygenase
TCA	cycle tricarboxylic acid cycle
TPP	thiamine pyrophosphate

Notes and references

1. Berg, IA.; Kockelkorn, D.; Ramos-Vera, WH.; Say, R.; Zarzycki, J.; Fuchs, G. Carbon Dioxide as Chemical Feedstock. Aresta, M., editor. WILEY-VCH Verlag GmbH & Co. KGaA; 2010. p. 33-53.
2. King GM, Weber CF. Nat Rev Microbiol. 2007; 5:107–118. [PubMed: 17224920]
3. Khalil MAK, Pinto JP, Shearer MJ. Chemosphere: Global Change Sci. 1999; 1:ix–xi.
4. Sato, T.; Atomi, H. Encyclopedia of Life Sciences. John Wiley and Sons, Ltd; Chicester: 2010.
5. Hügler M, Sievert SM. Annu Rev Mar Sci. 2011; 3:261–289.
6. Ragsdale, SW. Vitamins and Hormones. Litwack, G., editor. Elsevier, Inc; Amsterdam, The Netherlands: 2008. p. 293-324.
7. Topham, S. Ullmann's encyclopedia of Indudstrial Technology. Wiley-VCH Verlag GmbH & Co. KgaA; Weinheim: 2005.
8. Kirk-Othmer. Kirk-Othmer Encyclopedia of Chemical Technology. Wiley; 2004. p. 1-27.
9. Bierhals, J. Ullmann's Encyclopedia of Industrial Chemistry. Wiley-VCH; 2005.
10. Ryter SW, Otterbein LE. BioEssays. 2004; 26:270–280. [PubMed: 14988928]
11. Khalil MA, Rasmussen RA. Nature reviews Microbiology. 1994; 370:639–641.
12. Wuebbles, DJ.; Edmonds, J. Primer on Greenhouse Gases. Lewis Publishers; Chelsea, Mich: 1991.
13. Khalil MAK. Annu Rev Energy Environ. 1999; 24:645–661.
14. Ducklow, HW. Environmental Microbiology. Mitchell, R.; Gu, J., editors. Wiley-Blackwell; 2010.
15. Ragsdale SW. Incredible Anaerobes: From Physiology to Genomics to Fuels. 2008; 1125:129–136.
16. Ragsdale SW, Pierce E. Biochim Biophys Acta, Proteins Proteomics. 2008; 1784:1873–1898.
17. Drake HL, Gossner AS, Daniel SL. Incredible Anaerobes: From Physiology to Genomics to Fuels. 2008; 1125:100–128.
18. Martin W, Russell MJ. Philos Trans R Soc London, Ser B. 2007; 362:1887–1925. [PubMed: 17255002]
19. Brock, TD. Autotrophic Bacteria. Schlegel, HG.; Bowien, B., editors. Science Tech Publishers; Madison, WI: 1989. p. 499-512.
20. Svetlitchnyi V, Peschel C, Acker G, Meyer O. J Bacteriol. 2001; 183:5134–5144. [PubMed: 11489867]
21. Dubois MR, Dubois DL. Acc Chem Res. 2009; 42:1974–1982. [PubMed: 19645445]

22. Benson EE, Kubiak CP, Sathrum AJ, Smieja JM. Chem Soc Rev. 2009; 38:89–99. [PubMed: 19088968]
23. Groysman S, Holm RH. Biochemistry. 2009; 48:2310–2320. [PubMed: 19206188]
24. Evans DJ. Coord Chem Rev. 2005; 249:1582–1595.
25. Takuma M, Ohki Y, Tatsumi K. Inorg Chem. 2005; 44:6034–6043. [PubMed: 16097823]
26. Hofmann M, Kassube JK, Graf T. JBIC, J Biol Inorg Chem. 2005; 10:490–495.
27. Dobbek H, Gremer L, Meyer O, Huber R. Proc Natl Acad Sci U S A. 1999; 96:8884–8889. [PubMed: 10430865]
28. Beley M, Collin JP, Ruppert R, Sauvage JP. J Am Chem Soc. 1986; 108:7461–7467. [PubMed: 22283241]
29. Fisher B, Eisenberg R. J Am Chem Soc. 1980; 102:7361–7363.
30. Grodkowski J, Behar D, Neta P, Hambright P. J Phys Chem A. 1997; 101:248–254.
31. Behar D, Dhanasekaran T, Neta P, Hosten CM, Ejeh D, Hambright P, Fujita E. J Phys Chem A. 1998; 102:2870–2877.
32. Lieber CM, Lewis NS. J Am Chem Soc. 1984; 106:5033–5034.
33. Gattrell M, Gupta N, Co A. J Electroanal Chem. 2006; 594:1–19.
34. Laitar DS, Müller P, Sadighi JP. J Am Chem Soc. 2005; 127:17196–17197. [PubMed: 16332062]
35. Sayama K, Arakawa H. J Phys Chem. 1993; 97:531–533.
36. Wander SA, Miedaner A, Noll BC, Barkley RM, DuBois DL. Organometallics. 1996; 15:3360–3373.
37. Ettedgui J, Diskin-Posner Y, Weiner L, Neumann R. J Am Chem Soc. 2011; 133:188–190. [PubMed: 21158388]
38. Lu Z, Crabtree RH. J Am Chem Soc. 1995; 117:3994–3998.
39. Wang JB, Tsai DH, Huang TJ. J Catal. 2002; 208:370–380.
40. Zhou RX, Jiang XY, Mao JX, Zheng XM. Appl Catal, A. 1997; 162:213–222.
41. Sun JB, Tessier C, Holm RH. Inorg Chem. 2007; 46:2691–2699. [PubMed: 17346040]
42. Panda R, Berlinguette CP, Zhang Y, Holm RH. J Am Chem Soc. 2005; 127:11092–11101. [PubMed: 16076217]
43. Huang DG, Holm RH. J Am Chem Soc. 2010; 132:4693–4701. [PubMed: 20218565]
44. Doukov TI, Iverson TM, Seravalli J, Ragsdale SW, Drennan CL. Science. 2002; 298:567–572. [PubMed: 12386327]
45. Riordan CG. Journal of Biological Inorganic Chemistry. 2004; 9:542–549. [PubMed: 15221481]
46. Harrop TC, Mascharak PK. Coord Chem Rev. 2005; 249:3007–3024.
47. Krishnan R, Riordan CG. J Am Chem Soc. 2004; 126:4484–4485. [PubMed: 15070343]
48. Harrop TC, Olmstead MM, Mascharak PK. J Am Chem Soc. 2004; 126:14714–14715. [PubMed: 15535684]
49. Dougherty WG, Rangan K, O'Hagan MJ, Yap GPA, Riordan CG. J Am Chem Soc. 2008; 130:13510–13511. [PubMed: 18800791]
50. Lee CM, Chen CH, Liao FX, Hu CH, Lee GH. J Am Chem Soc. 2010; 132:9256–9258. [PubMed: 20568755]
51. Matsumoto T, Ito M, Kotera M, Tatsumi K. Dalton Trans. 2010; 39:2995–2997. [PubMed: 20221531]
52. Ito M, Kotera M, Matsumoto T, Tatsumi K. Proc Natl Acad Sci U S A. 2009; 106:11862–11866. [PubMed: 19584250]
53. Mathrubootham V, Thomas J, Staples R, McCraken J, Shearer J, Hegg EL. Inorg Chem. 2010; 49:5393–5406. [PubMed: 20507077]
54. Frey, PA.; Hegeman, AD. Enzymatic Reaction Mechanisms. Oxford University Press; Oxford, New York: 2007.
55. Tittmann K. FEBS J. 2009; 276:2454–2468. [PubMed: 19476487]
56. Ragsdale SW. Chem Rev. 2003; 103:2333–2346. [PubMed: 12797832]

57. Shepard EM, Duffus BR, George SJ, McGlynn SE, Challand MR, Swanson KD, Roach PL, Cramer SP, Peters JW, Broderick JB. J Am Chem Soc. 2010; 132:9247–9249. [PubMed: 20565074]
58. Kim HP, Ryter SW, Choi AM. Annu Rev Pharmacol. 2006; 46:411–449.
59. Bauer I, Debeyer A, Tshisuaka B, Fetzner S, Lingens F. FEMS Microbiol Lett. 1994; 117:299–304.
60. Oka T, Simpson FJ. Biochem Biophys Res Commun. 1971; 43:1–5. [PubMed: 5579942]
61. Schirmer A, Rude MA, Li XZ, Popova E, del Cardayre SB. Science. 2010; 329:559–562. [PubMed: 20671186]
62. Wray JW, Abeles RH. Journal of Biological Chemistry. 1993; 268:21466–21469. [PubMed: 8407993]
63. Yamamoto I, Saiki T, Liu SM, Ljungdahl LG. Journal of Biological Chemistry. 1983; 258:1826–1832. [PubMed: 6822536]
64. Jollie DR, Lipscomb JD. Journal of Biological Chemistry. 1991; 266:21853–21863. [PubMed: 1657982]
65. Asano Y, Sekigawa T, Inukai H, Nakazawa A. J Bacteriol. 1988; 170:3189–3193. [PubMed: 3384805]
66. Jormakka M, Byrne B, Iwata S. Curr Opin Struct Biol. 2003; 13:418–423. [PubMed: 12948771]
67. Brondino CD, Passeggi MCG, Caldeira J, Almendra MJ, Feio MJ, Moura JJG, Moura I. JBIC, J Biol Inorg Chem. 2004; 9:145–151.
68. Yamamoto I, Saiki T, Liu SM, Ljungdahl LG. Journal of Biological Chemistry. 1983; 258:1826–1832. [PubMed: 6822536]
69. Schauer NL, Ferry JG, Honek JF, Ormejohnson WH, Walsh C. Biochemistry. 1986; 25:7163–7168. [PubMed: 3801411]
70. Ruiz-Herrera J, Demoss JA. Journal of Bacteriology. 1969; 99:720–729. [PubMed: 4905536]
71. Meyer O, Schlegel HG. Arch Microbiol. 1978; 118:35–43. [PubMed: 697501]
72. Kistner A. Proceedings of the Koninklijke Nederlandse Akademie van Wetenschappen, Series C. 1954; 57:186–195.
73. King GM, Weber CF. Nat Rev Microbiol. 2007; 5:107–118. [PubMed: 17224920]
74. Schubel U, Kraut M, Morsdorf G, Meyer O. J Bacteriol. 1995; 177:2197–2203. [PubMed: 7721710]
75. Dobbek H, Gremer L, Kiefersauer R, Huber R, Meyer O. Proc Natl Acad Sci U S A. 2002; 99:15971–15976. [PubMed: 12475995]
76. Gnida M, Ferner R, Gremer L, Meyer O, Meyer-Klaucke W. Biochemistry. 2002; 42:222–230. [PubMed: 12515558]
77. Resch M, Dobbek H, Meyer O. JBIC, J Biol Inorg Chem. 2005; 10:518–528.
78. Eliot AC, Kirsch JF. Annu Rev Biochem. 2004; 73:383–415. [PubMed: 15189147]
79. Ishikita H. FEBS Lett. 2010; 584:3464–3468. [PubMed: 20621098]
80. Knappe J, Wagner AF. Adv Protein Chem. 2001; 58:277–315. [PubMed: 11665490]
81. Nikolau BJ, Ohlrogge JB, Wurtele ES. Arch Biochem Biophys. 2003; 414:211–222. [PubMed: 12781773]
82. BRENDA Enzyme Database. 2011. http://www.brenda-enzymes.info/index.php4
83. Boyd JM, Ellsworth H, Ensign SA. J Biol Chem. 2004; 279:46644–46651. [PubMed: 15337755]
84. Charles AM, Sykora Y. Antonie van Leeuwenhoek. 1992; 62:155–165. [PubMed: 1416912]
85. Wong CM, Marcocci L, Liu L, Suzuki YJ. Antioxid Redox Signaling. 2010; 12:393–404.
86. Ragsdale SW. Crit Rev Biochem Mol Biol. 2004; 39:165–195. [PubMed: 15596550]
87. Santiago B, Schübel U, Egelseer C, Meyer O. Gene. 1999; 236:115–124. [PubMed: 10433972]
88. Pelzmann A, Ferner M, Gnida M, Meyer-Klaucke W, Maisel T, Meyer O. J Biol Chem. 2009; 284:9578–9586. [PubMed: 19189964]
89. Hanzelmann P, Meyer O. Eur J Biochem. 1998; 255:755–765. [PubMed: 9738918]

90. Hänzelmann P, Dobbek H, Gremer L, Huber R, Meyer O. J Mol Biol. 2000; 301:1221–1235. [PubMed: 10966817]
91. Hofmann M, Kassube J, Graf T. JBIC, J Biol Inorg Chem. 2005; 10:490–495.
92. Siegbahn PEM, Shestakov AF. J Comput Chem. 2005; 26:888–898. [PubMed: 15834924]
93. Daniels L, Fuchs G, Thauer RK, Zeikus JG. J Bacteriol. 1977; 132:118–126. [PubMed: 21159]
94. Gottwald M, Andreesen JR, LeGall J, Ljungdahl LG. J Bacteriol. 1975; 122:325–328. [PubMed: 1123319]
95. Diekert GB, Thauer RK. J Bacteriol. 1978; 136:597–606. [PubMed: 711675]
96. Kerby R, Zeikus JG. Curr Microbiol. 1983; 8:27–30.
97. Uffen RL. Proc Natl Acad Sci U S A. 1976; 73:3298–3302. [PubMed: 1067620]
98. Uffen RL, Wolfe RS. J Bacteriol. 1970; 104:462–472. [PubMed: 5473903]
99. Yagi T. Biochim Biophys Acta. 1958; 30:194–195. [PubMed: 13584419]
100. Yagi T. Journal of Biochemistry. 1959; 46:949–955.
101. Yagi T, Tamiya N. Biochim Biophys Acta. 1962; 65:508–509. [PubMed: 14002201]
102. Zavarzin GA, Nozhevnikova AN. Microb Ecol. 1977; 3:305–326. [PubMed: 24233667]
103. Thauer RK, Fuchs G, Käuefer B, Schnttker U. Eur J Biochem. 1974; 45:343–349. [PubMed: 4152801]
104. Fuchs G, Schnitker U, Thauer RK. Eur J Biochem. 1974; 49:111–115. [PubMed: 4459138]
105. Chappelle EW. Biochim Biophys Acta. 1962; 62:45–62. [PubMed: 13878211]
106. Zhang B, Hemann CF, Hille R. J Biol Chem. 2010; 285:12571–12578. [PubMed: 20178978]
107. Wilcoxen J, Zhang B, Hille R. Biochemistry. 2011; 50:1910–1916. [PubMed: 21275368]
108. Henstra AM, Stams AJM. Appl Environ Microbiol. 2004; 70:7236–7240. [PubMed: 15574922]
109. Wu M, Ren Q, Durkin AS, Daugherty SC, Brinkac LM, Dodson RJ, Madupu R, Sullivan SA, Kolonay JF, Haft DH, Nelson WC, Tallon LJ, Jones KM, Ulrich LE, Gonzalez JM, Zhulin IB, Robb FT, Eisen JA. PLoS Genet. 2005; 1:563–574.
110. Soboh B, Linder D, Hedderich R. Eur J Biochem. 2002; 269:5712–5721. [PubMed: 12423371]
111. Morton, TA. University of Georgia; 1991.
112. Roberts DL, James-Hagstrom JE, Smith DK, Gorst CM, Runquist JA, Baur JR, Haase FC, Ragsdale SW. Proc Natl Acad Sci U S A. 1989; 86:32–36. [PubMed: 2911576]
113. Pierce E, Xie G, Barabote RD, Saunders E, Han CS, Detter JC, Richardson P, Brettin TS, Das A, Ljungdahl LG, Ragsdale SW. Environ Microbiol. 2008; 10:2550–2573. [PubMed: 18631365]
114. Maupin-Furlow JA, Ferry JG. J Bacteriol. 1996; 178:6849–6856. [PubMed: 8955306]
115. Grahame D, Gencic S, DeMoll E. Arch Microbiol. 2005; 184:32–40. [PubMed: 16044263]
116. Ragsdale SW, Clark JE, Ljungdahl LG, Lundie LL, Drake HL. J Biol Chem. 1983; 258:2364–2369. [PubMed: 6687389]
117. Ragsdale SW, Wood HG. Journal of Biological Chemistry. 1985; 260:3970–3977. [PubMed: 2984190]
118. Terlesky KC, Nelson MJ, Ferry JG. J Bacteriol. 1986; 168:1053–1058. [PubMed: 3023296]
119. Grahame DA. Journal of Biological Chemistry. 1991; 266:22227–22233. [PubMed: 1939246]
120. Peinemann S, Müller V, Blaut M, Gottschalk G. J Bacteriol. 1988; 170:1369–1372. [PubMed: 3343222]
121. Krzycki JA, Lehman LJ, Zeikus JG. J Bacteriol. 1985; 163:1000–1006. [PubMed: 3928595]
122. Fischer R, Thauer RK. FEBS Lett. 1988; 228:249–253.
123. Fischer R, Thauer RK. FEBS Lett. 1990; 269:368–372. [PubMed: 15452975]
124. Roberts GP, Youn H, Kerby RL. Microbiol Mol Biol Rev. 2004; 68:453–473. [PubMed: 15353565]
125. Komori H, Inagaki S, Yoshioka S, Aono S, Higuchi Y. J Mol Biol. 2007; 367:864–871. [PubMed: 17292914]
126. Youn H, Kerby RL, Conrad M, Roberts GP. J Bacteriol. 2004; 186:1320–1329. [PubMed: 14973040]
127. Kerby RL, Youn H, Roberts GP. J Bacteriol. 2008; 190:3336–3343. [PubMed: 18326575]

128. Drennan CL, Heo J, Sintchak MD, Schreiter E, Ludden PW. Proc Natl Acad Sci U S A. 2001; 98:11973–11978. [PubMed: 11593006]
129. Dobbek H, Svetlitchnyi V, Gremer L, Huber R, Meyer O. Science. 2001; 293:1281–1285. [PubMed: 11509720]
130. Darnault C, Volbeda A, Kim EJ, Legrand P, Vernede X, Lindahl PA, Fontecilla-Camps JC. Nat Struct Biol. 2003; 10:271–279. [PubMed: 12627225]
131. Gong W, Hao B, Wei Z, Ferguson DJ, Tallant T, Krzycki JA, Chan MK. Proc Natl Acad Sci U S A. 2008; 105:9558–9563. [PubMed: 18621675]
132. Jeoung JH, Dobbek H. Science. 2007; 318:1461–1464. [PubMed: 18048691]
133. Kung Y, Doukov TI, Seravalli J, Ragsdale SW, Drennan CL. Biochemistry. 2009; 48:7432–7440. [PubMed: 19583207]
134. Kerby RL, Ludden PW, Roberts GP. J Bacteriol. 1997; 179:2259–2266. [PubMed: 9079911]
135. Jeon WB, Cheng JJ, Ludden PW. J Biol Chem. 2001; 276:38602–38609. [PubMed: 11507093]
136. Drake HL, Hu SI, Wood HG. Journal of Biological Chemistry. 1980; 255:7174–7180. [PubMed: 6893049]
137. Diekert G, Thauer RK. FEMS Microbiol Lett. 1980; 7:187–189.
138. Lindahl PA, Münck E, Ragsdale SW. Journal of Biological Chemistry. 1990; 265:3873–3879. [PubMed: 2154491]
139. Kumar M, Lu WP, Liu L, Ragsdale SW. J Am Chem Soc. 1993; 115:11646–11647.
140. Seravalli J, Kumar M, Lu WP, Ragsdale SW. Biochemistry. 1995; 34:7879–7888. [PubMed: 7794899]
141. Kung Y, Drennan CL. Curr Opin Chem Biol. 2010; 15:276–283. [PubMed: 21130022]
142. Chen JY, Huang S, Seravalli J, Gutzman H, Swartz DJ, Ragsdale SW, Bagley KA. Biochemistry. 2003; 42:14822–14830. [PubMed: 14674756]
143. Ha SW, Korbas M, Klepsch M, Meyer-Klaucke W, Meyer O, Svetlitchnyi V. J Biol Chem. 2007; 282:10639–10646. [PubMed: 17277357]
144. Jeoung JH, Dobbek H. J Am Chem Soc. 2009; 131:9922–9923. [PubMed: 19583208]
145. Ensign SA, Hyman MR, Ludden PW. Biochemistry. 1989; 28:4973–4979. [PubMed: 2504285]
146. Anderson ME, Lindahl PA. Biochemistry. 1994; 33:8702–8711. [PubMed: 8038160]
147. Qiu D, Kumar M, Ragsdale SW, Spiro TG. J Am Chem Soc. 1996; 118:10429–10435.
148. Kim EJ, Feng J, Bramlett MR, Lindahl PA. Biochemistry. 2004; 43:5728–5734. [PubMed: 15134447]
149. Bertini, I.; Luchinat, C. Bioinorganic Chemistry. Bertini, I.; Gray, HB.; Lippard, SJ.; Valentine, JS., editors. University Science Books; Mill Valley, CA: 1994. p. 37-106.
150. Lindahl PA. Biochemistry. 2002; 41:2097–2105. [PubMed: 11841199]
151. Seravalli J, Kumar M, Lu WP, Ragsdale SW. Biochemistry. 1997; 36:11241–11251. [PubMed: 9287167]
152. Shin W, Lee S, Shin J, Lee S, Kim Y. J Am Chem Soc. 2003; 125:14688–14689. [PubMed: 14640627]
153. Smith ET, Ensign SA, Ludden PW, Feinberg BA. Biochemical Journal. 1992; 285:181–185. [PubMed: 1637298]
154. Parkin A, Seravalli J, Vincent KA, Ragsdale SW, Armstrong FA. J Am Chem Soc. 2007; 129:10328–10329. [PubMed: 17672466]
155. Koppenol WH, Rush JD. J Phys Chem. 1987; 91:4429–4430.
156. Lazarus O, Woolerton TW, Parkin A, Lukey MJ, Reisner E, Seravalli J, Pierce E, Ragsdale SW, Sargent F, Armstrong FA. J Am Chem Soc. 2009; 131:14154–14155. [PubMed: 19807170]
157. Woolerton TW, Sheard S, Reisner E, Pierce E, Ragsdale SW, Armstrong FA. J Am Chem Soc. 2010; 132:2132–2133. [PubMed: 20121138]
158. Cypionka H, Meyer O. Arch Microbiol. 1983; 135:293–298.
159. Cypionka H, Meyer O. J Bacteriol. 1983; 156:1178–1187. [PubMed: 6315679]
160. Cypionka H, van Verseveld HW, Stouthamer AH. FEMS Microbiol Lett. 1984; 22:209–213.

161. Podzuweit HG, Arp DJ. Arch Microbiol. 1987; 146:332–337.
162. Drake HL, Hu SI, Wood HG. Journal of Biological Chemistry. 1981; 256:11137–11144. [PubMed: 7287757]
163. Ljungdahl L, Brewer JM, Neece SH, Fairwell T. Journal of Biological Chemistry. 1970; 245:4791–4797. [PubMed: 5456151]
164. Hugenholtz J, Ivey DM, Ljungdahl LG. Journal of Bacteriology. 1987; 169:5845–5847. [PubMed: 3680181]
165. Das A, Hugenholtz J, Van Halbeek H, Ljungdahl LG. J Bacteriol. 1989; 171:5823–5829. [PubMed: 2808299]
166. Fuchs G. FEMS Microbiol Lett. 1986; 39:181–213.
167. Ivey DM, Ljungdahl LG. J Bacteriol. 1986; 165:252–257. [PubMed: 2867087]
168. Das A, Ljungdahl L. J Bacteriol. 1997; 179:3746–3755. [PubMed: 9171425]
169. Hugenholtz J, Ljungdahl LG. J Bacteriol. 1989; 171:2873–2875. [PubMed: 2708323]
170. Dangel W, Schulz H, Diekert G, König H, Fuchs G. Arch Microbiol. 1987; 148:52–56.
171. Müller V. Appl Environ Microbiol. 2003; 69:6345–6353. [PubMed: 14602585]
172. Heise R, Müller V, Gottschalk G. J Bacteriol. 1989; 171:5473–5478. [PubMed: 2507527]
173. Heise R, Müller V, Gottschalk G. FEMS Microbiol Lett. 1993; 112:261–268.
174. Reidlinger J, MÜLler V. Eur J Biochem. 1994; 223:275–283. [PubMed: 8033902]
175. Fritz M, Klyszejko AL, Morgner N, Vonck J, Brutschy B, Müller DJ, Meier T, Müller V. FEBS J. 2008; 275:1999–2007. [PubMed: 18355313]
176. Fritz M, Müller V. FEBS J. 2007; 274:3421–3428. [PubMed: 17555523]
177. Imkamp F, Biegel E, Jayamani E, Buckel W, Müller V. J Bacteriol. 2007; 189:8145–8153. [PubMed: 17873051]
178. Biegel E, Schmidt S, Müller V. Environ Microbiol. 2009; 11:1438–1443. [PubMed: 19222539]
179. Biegel E, Müller V. J Biol Chem. 2011; 286:6080–6084. [PubMed: 21173152]
180. Furdui C, Ragsdale SW. J Biol Chem. 2000; 275:28494–28499. [PubMed: 10878009]
181. Bock AK, Kunow J, Glasemacher J, Schönheit P. Eur J Biochem. 1996; 237:35–44. [PubMed: 8620891]
182. Simpson, PG.; Whitman, WB. Methanogenesis: Ecology Physiology, Biochemistry & Genetics. Ferry, JG., editor. Chapman & Hall; London: 1993. p. 445-472.
183. Yoon KS, Hille R, Hemann C, Tabita FR. J Biol Chem. 1999; 274:29772–29778. [PubMed: 10514453]
184. Horner DS, Hirt RP, Embley TM. Mol Biol Evol. 1999; 16:1280–1291. [PubMed: 10486982]
185. Löfmark S, Edlund C, Nord C. Clin Infect Dis. 2010; 50(Suppl 1):S16–23. [PubMed: 20067388]
186. Hughes NJ, Chalk PA, Clayton CL, Kelly DJ. J Bacteriol. 1995; 177:3953–3959. [PubMed: 7608066]
187. Adams MWW, Kletzin A. Adv Protein Chem. 1996; 48:101–180. [PubMed: 8791625]
188. Zhang Q, Iwasaki T, Wakagi T, Oshima T. J Biochem Tokyo. 1996; 120:587–599. [PubMed: 8902625]
189. Kletzin A, Adams MWW. J Bacteriol. 1996; 178:248–257. [PubMed: 8550425]
190. Chabrière E, Charon MH, Volbeda A, Pieulle L, Hatchikian EC, Fontecilla-Camps JC. Nat Struct Biol. 1999; 6:182–190. [PubMed: 10048931]
191. Pieulle L, Chabrière E, Hatchikian C, FontecillaCamps JC, Charon MH. Acta Crystallogr, Sect D: Biol Crystallogr. 1999; 55:329–331. [PubMed: 10089441]
192. Furdui C, Ragsdale SW. Biochemistry. 2002; 41:9921–9937. [PubMed: 12146957]
193. Chabrière E, Vernede X, Guigliarelli B, Charon MH, Hatchikian EC, Fontecilla-Camps JC. Science. 2001; 294:2559–2563. [PubMed: 11752578]
194. Mansoorabadi SO, Seravalli J, Furdui C, Krymov V, Gerfen GJ, Begley TP, Melnick J, Ragsdale SW, Reed GH. Biochemistry. 2006; 45:7122–7131. [PubMed: 16752902]
195. Menon S, Ragsdale SW. Biochemistry. 1997; 36:8484–8494. [PubMed: 9214293]

196. Tittmann K, Golbik R, Ghisla S, Hubner G. Biochemistry. 2000; 39:10747–10754. [PubMed: 10978159]
197. Tittmann K, Wille G, Golbik R, Weidner A, Ghisla S, Hubner G. Biochemistry. 2005; 44:13291–13303. [PubMed: 16201755]
198. Hu SI, Pezacka E, Wood HG. J Biol Chem. 1984; 259:8892–8897. [PubMed: 6746629]
199. Ragsdale SW, Lindahl PA, Münck E. J Biol Chem. 1987; 262:14289–14297. [PubMed: 2821001]
200. Seravalli J, Zhao S, Ragsdale SW. Biochemistry. 1999; 38:5728–5735. [PubMed: 10231523]
201. Zhao SY, Ragsdale SW. Biochemistry. 1996; 35:2476–2481. [PubMed: 8652591]
202. Zhao S, Roberts DL, Ragsdale SW. Biochemistry. 1995; 34:15075–15083. [PubMed: 7578120]
203. Doukov TI, Hemmi H, Drennan CL, Ragsdale SW. J Biol Chem. 2007; 282:6609–6618. [PubMed: 17172470]
204. Seravalli J, Shoemaker RK, Sudbeck MJ, Ragsdale SW. Biochemistry. 1999; 38:5736–5745. [PubMed: 10231524]
205. Lu WP, Harder SR, Ragsdale SW. Journal of Biological Chemistry. 1990; 265:3124–3133. [PubMed: 2303444]
206. Menon S, Ragsdale SW. J Biol Chem. 1999; 274:11513–11518. [PubMed: 10206956]
207. Bender G, Stich TA, Yan L, Britt RD, Cramer SP, Ragsdale SW. Biochemistry. 2010; 49:7516–7523. [PubMed: 20669901]
208. Menon S, Ragsdale SW. Biochemistry. 1996; 35:12119–12125. [PubMed: 8810918]
209. Zinder SH, Anguish T. Applied and Environmental Microbiology. 1992; 58:3323–3329. [PubMed: 16348788]
210. Seravalli J, Ragsdale SW. Biochemistry. 2000; 39:1274–1277. [PubMed: 10684606]
211. Maynard EL, Lindahl PA. J Am Chem Soc. 1999; 121:9221–9222.
212. Doukov TI, Blasiak LC, Seravalli J, Ragsdale SW, Drennan CL. Biochemistry. 2008; 47:3474–3483. [PubMed: 18293927]
213. Darnault C, Volbeda A, Kim EJ, Legrand P, Vernede X, Lindahl PA, Fontecilla-Camps JC. Nat Struct Biol. 2003; 10:271–279. [PubMed: 12627225]
214. Tan XS, Lindahl PA. JBIC, J Biol Inorg Chem. 2008; 13:771–778.
215. Gong W, Hao B, Wei Z, Ferguson DJ, Tallant T, Krzycki JA, Chan MK. Proc Natl Acad Sci U S A. 2008; 105:9558–9563. [PubMed: 18621675]
216. Ragsdale SW. J Inorg Biochem. 2007; 101:1657–1666. [PubMed: 17716738]
217. Drennan CL, Doukov TI, Ragsdale SW. JBIC, J Biol Inorg Chem. 2004; 9:511–515.
218. Ragsdale SW, Ljungdahl LG, DerVartanian DV. Biochem Biophys Res Commun. 1982; 108:658–663. [PubMed: 6293499]
219. Ragsdale SW, Wood HG, Antholine WE. Proc Natl Acad Sci U S A. 1985; 82:6811–6814. [PubMed: 2995986]
220. Fan CL, Gorst CM, Ragsdale SW, Hoffman BM. Biochemistry. 1991; 30:431–435. [PubMed: 1846295]
221. Seravalli J, Gu WW, Tam A, Strauss E, Begley TP, Cramer SP, Ragsdale SW. Proc Natl Acad Sci U S A. 2003; 100:3689–3694. [PubMed: 12589021]
222. Gencic S, Grahame DA. J Biol Chem. 2003; 278:6101–6110. [PubMed: 12464601]
223. Bramlett MR, Tan X, Lindahl PA. J Am Chem Soc. 2003; 125:9316–9317. [PubMed: 12889960]
224. Seravalli J, Xiao YM, Gu WW, Cramer SP, Antholine WE, Krymov V, Gerfen GJ, Ragsdale SW. Biochemistry. 2004; 43:3944–3955. [PubMed: 15049702]
225. Svetlitchnyi V, Dobbek H, Meyer-Klaucke W, Meins T, Thiele B, Romer P, Huber R, Meyer O. Proc Natl Acad Sci U S A. 2004; 101:446–451. [PubMed: 14699043]
226. Tan XS, Bramlett MR, Lindahl PA. J Am Chem Soc. 2004; 126:5954–5955. [PubMed: 15137746]
227. Loke HK, Lindahl PA. J Inorg Biochem. 2003; 93:33–40. [PubMed: 12538050]
228. Brunold TC. JBIC, J Biol Inorg Chem. 2004; 9:533–541.
229. Lindahl PA. Journal of Biological Inorganic Chemistry. 2004; 9:516–524. [PubMed: 15221478]

230. Vobeda A, Fontecilla-Camps JC. J Biol Inorg Chem. 2004; 9:525–532. [PubMed: 15221479]
231. Seravalli J, Ragsdale SW. J Biol Chem. 2008; 283:8384–8394. [PubMed: 18203715]
232. Barondeau DP, Lindahl PA. J Am Chem Soc. 1997; 119:3959–3970.
233. George SJ, Seravalli J, Ragsdale SW. J Am Chem Soc. 2005; 127:13500–13501. [PubMed: 16190705]
234. Lu WP, Ragsdale SW. Journal of Biological Chemistry. 1991; 266:3554–3564. [PubMed: 1995618]
235. Bhaskar B, DeMoll E, Grahame DA. Biochemistry. 1998; 37:14491–14499. [PubMed: 9772177]
236. Bender G, Ragsdale SW. Biochemistry. 2011; 50:276–286. [PubMed: 21141812]
237. Lebertz H, Simon H, Courtney LF, Benkovic SJ, Zydowsky LD, Lee K, Floss HD. J Am Chem Soc. 1987; 109:3173–3174.
238. Hegg EL. Acc Chem Res. 2004; 37:775–783. [PubMed: 15491124]
239. Tan X, Martinho M, Stubna A, Lindahl PA, Munck E. J Am Chem Soc. 2008; 130:6712–6713. [PubMed: 18459773]
240. Bramlett MR, Stubna A, Tan XS, Surovtsev IV, Munck E, Lindahl PA. Biochemistry. 2006; 45:8674–8685. [PubMed: 16834342]
241. Gencic S, Grahame DA. Biochemistry. 2008; 47:5544–5555. [PubMed: 18442256]
242. Ragsdale SW, Wood HG. Journal of Biological Chemistry. 1985; 260:3970–3977. [PubMed: 2984190]
243. Shanmugasundaram T, Kumar GK, Wood HG. Biochemistry. 1988; 27:6499–6503. [PubMed: 3219350]
244. Morton TA, Runquist JA, Ragsdale SW, Shanmugasundaram T, Wood HG, Ljungdahl LG. Journal of Biological Chemistry. 1991; 266:23824–23828. [PubMed: 1748656]
245. Seravalli J, Kumar M, Ragsdale SW. Biochemistry. 2002; 41:1807–1819. [PubMed: 11827525]
246. Gorst CM, Ragsdale SW. Journal of Biological Chemistry. 1991; 266:20687–20693. [PubMed: 1657934]
247. George SJ, Seravalli J, Ragsdale SW. J Am Chem Soc. 2005; 127:13500–13501. [PubMed: 16190705]
248. Maynard EL, Sewell C, Lindahl PA. J Am Chem Soc. 2001; 123:4697–4703. [PubMed: 11457278]
249. Tan XS, Sewell C, Lindahl PA. J Am Chem Soc. 2002; 124:6277–6284. [PubMed: 12033855]

Biographies

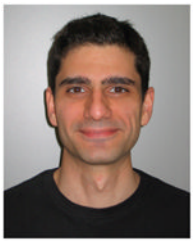

Gunes Bender is from Ankara, Turkey. He studied Biology and Chemistry at Swarthmore College, PA. Then he attended the Biophysics doctoral degree program at University of Wisconsin-Madison, where he discovered his interest in enzymes and electron paramagnetic resonance. He obtained his PhD in 2008 under the guidance of George H. Reed. In the recent years, as a postdoctoral research fellow, he has been studying the enzymes of Wood-Ljungdahl pathway in acetogens in the laboratory of Stephen W. Ragsdale.

Elizabeth Pierce is a PhD student at the University of Michigan in the laboratory of Stephen Ragsdale. She grew up in Missouri, received a bachelor of science degree in biology from Missouri Western State University and a master of science in biochemistry from the University of Nebraska-Lincoln. Her work in Dr Ragsdale's lab has included studies on metabolism of oxalate in Moorella thermoacetica by a thiamine pyrophosphate dependent oxalate oxidoreductase, annotation of the M. thermoacetica genome sequence, and work on CODH and ACS.

Jeffrey Hill grew up in Lexington, Kentucky. He served six years in the United States Navy including four years onboard the USS Parche SSN-683, the most decorated ship in US Naval history, as a nuclear propulsion plant operator and an engineering laboratory technician. He was honorably discharged in 2000. He received his Bachelor's degree in chemistry from Missouri State University in 2008. He joined the Chemical Biology Doctoral Program at the University of Michigan in the fall of 2009. His current studies in the Ragsdale lab focus on the corrinoid iron–sulfur protein, a key component of the Wood-Ljungdahl pathway.

Joseph Darty is from Southeastern Michigan. He earned his Bachelors of Science and Masters of Science degrees in Chemistry at the University of North Carolina at Greensboro, where he studied physical organic chemistry related to rotational barriers of hindered molecules by NMR. He earned his PhD in Biochemistry (2008) in the Chemistry and Biochemistry program at the University of Texas at Austin under Chris Whitman, studying protein evolution and engineering using random and directed evolution techniques. Presently, as a postdoctoral research fellow, he is studying protein interactions and substrate channeling in the Wood-Ljungdahl pathway in the Ragsdale laboratory.

Stephen W. Ragsdale is Professor of Biological Chemistry at the University of Michigan. His research focuses on enzymes of the global carbon cycle that are key to biological methane formation and CO_2/CO fixation. His laboratory has shown that these enzymes utilize mechanisms involving organometallic intermediates, metal centers acting as nucleophiles, and gas channels. He also is studying metabolic regulation in mammals involving redox, heme and reactive gaseous molecules (e.g., CO, NO). He is a Fellow of the American Society for Microbiology and a Fellow of the American Association for the Advancement of Science.

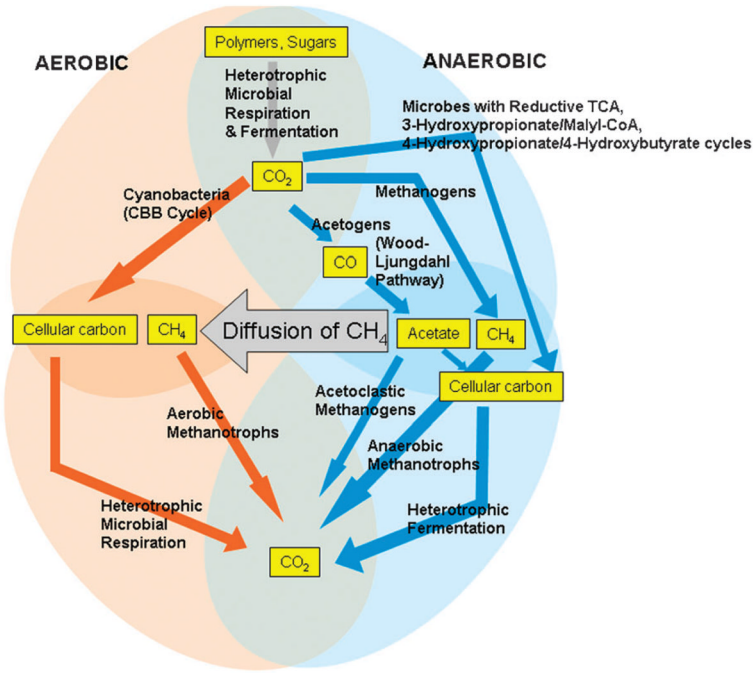

Fig. 1.
Microorganisms that contribute to the carbon cycle.

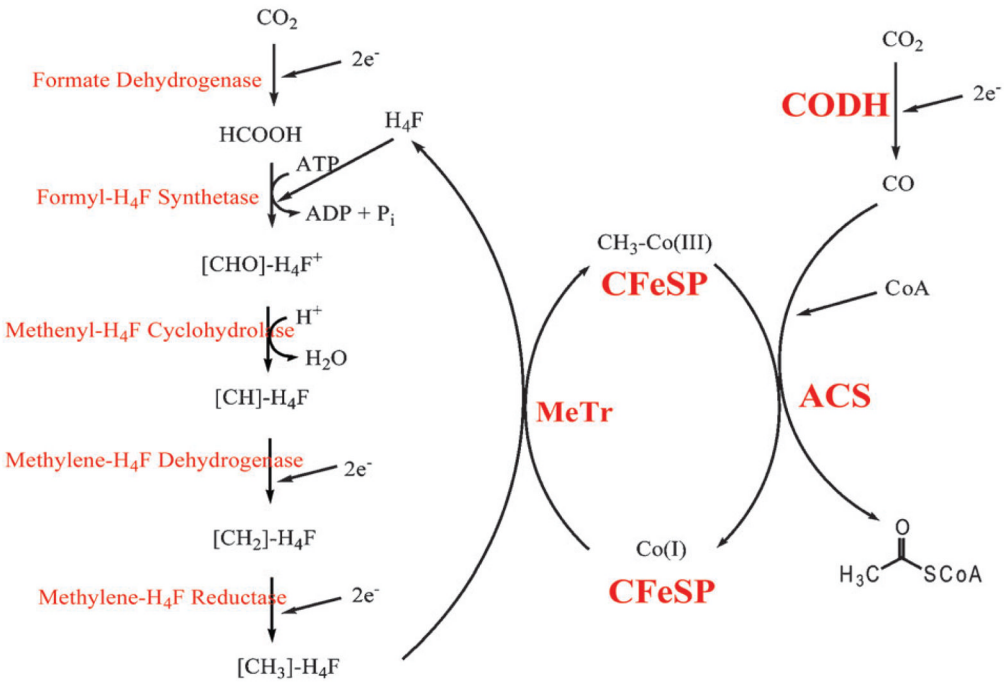

Fig. 2.

The Wood-Ljungdahl pathway. On the left hand side, the Methyl branch is depicted where 1 mol of CO_2 is reduced to methyl-tetrahydrofolate. On the right is the Carbonyl branch where acetyl-CoA is synthesized.

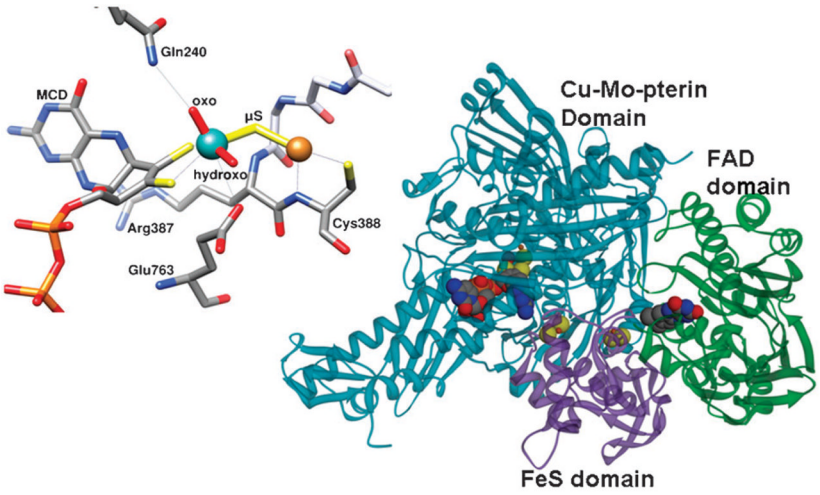

Fig. 3.

The structure of a heterotrimer of aerobic CODH and the active site of the aerobic CODH from *Oligotropha carboxydovorans* (pdb: 1N5W). The molybdenum atom is shown in cyan, the copper atom in orange. Contacts to both metals within 3.2 Å are shown as light grey lines. For Mo, these include the side chains of Gln 763 (3.16Å) and the sulfur atoms of the MCD cofactor (2.45Å and 2.49Å). For Cu, these include the backbone N (3.14 Å) and sulfur (2.22 Å) of Cys388. The cytosine portion of the MCD cofactor is not shown. The overall structure of a monomer on the right shows the Cu-Mo-pterin domain in blue, the Fe_2S_2 domain in pink, and the FAD domain in green.

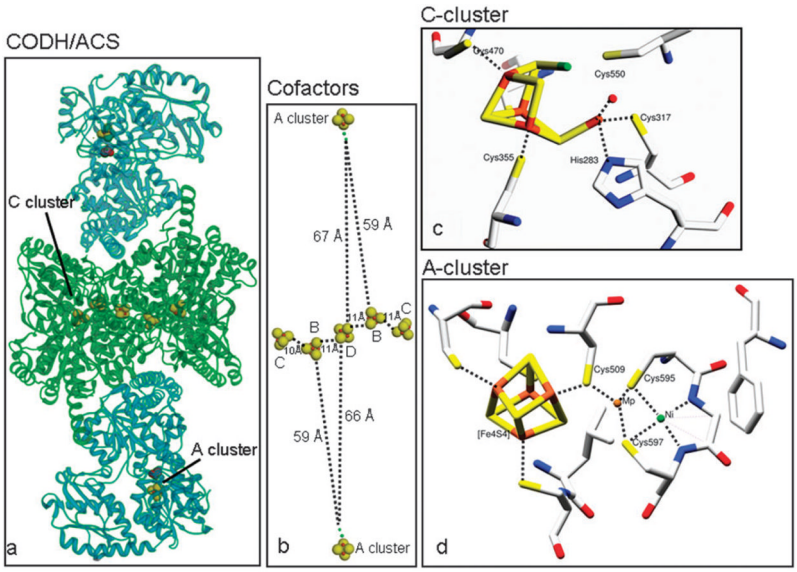

Fig. 4.

Overall structure of the bifunctional CODH/ACS from *Moorella thermoacetica* (pdb:1MJG) is shown in (a). The distances between the cofactors, Clusters B, C and D are close enough for electron transfer to happen inside the CODH subunit, but not to the A cluster, which is 59–67 Å away (b). In panel c, depicting the active site of CODH II from *Carboxydothermus hydrogenoformans*, from (pdb:1JJY), the nickel atom is shown in green, iron atoms in brown, and sulfur atoms in yellow. All residues coordinating the metal cluster are shown. In lower right panel d, where active site of ACS from *Moorella thermoacetica* (pdb:1MJG) is depicted, the Fe_4S_4 cluster, the proximal and distal metals, and the cysteine ligands are shown. In this crystal structure, the proximal position was occupied with Cu instead of the native Ni residue.[44] Zn can also be found in the M_p site.

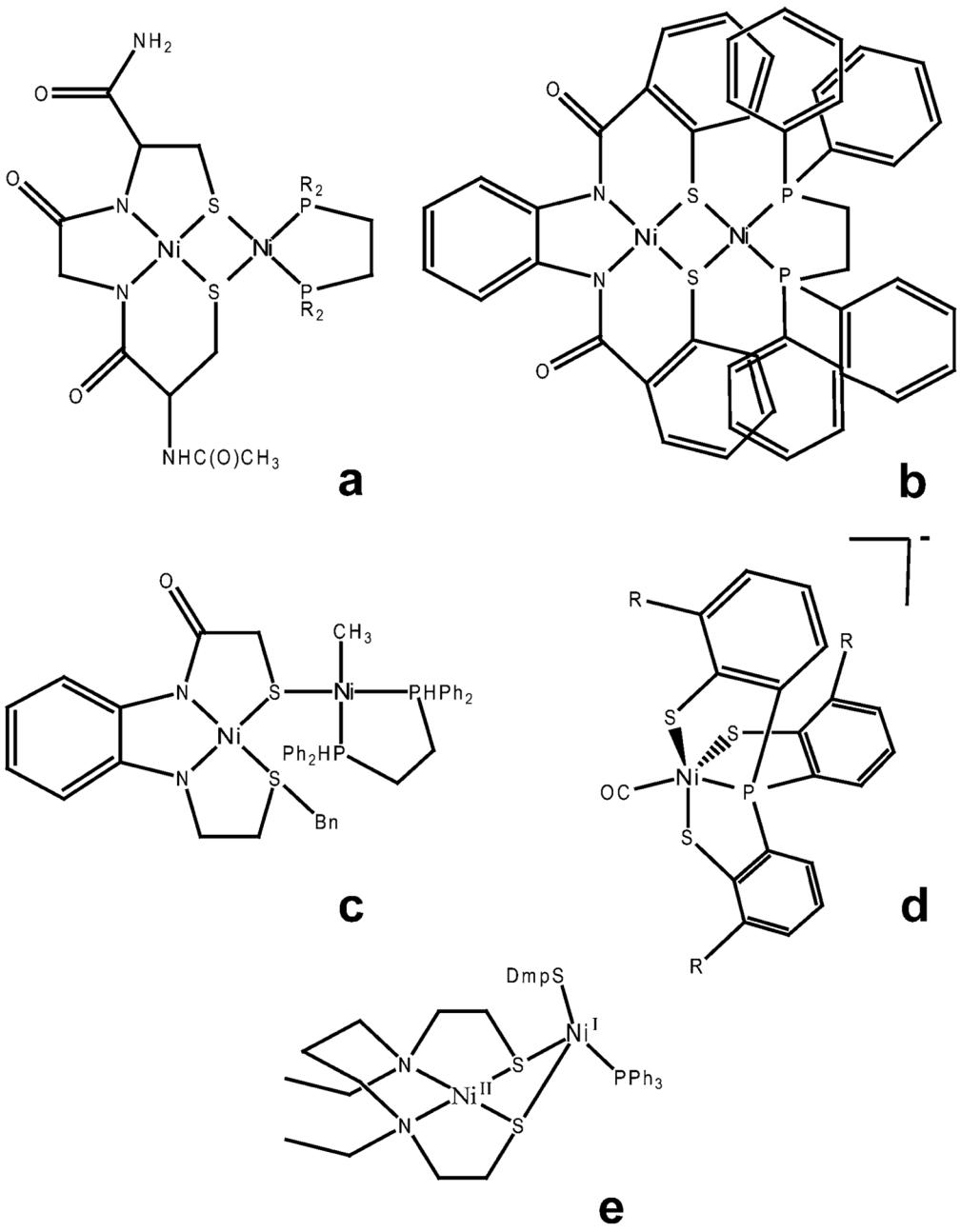

Fig. 5.

Examples of inorganic A-cluster mimics from the literature with similar properties to the A-cluster. a: [(CysGlyCys)Ni]Ni(dppe),[47] b: [Ni^{II}(dppe)Ni^{II}(PhPepS)],[48] c: Methyl-Ni complex,[49] d: [PPN][Ni^{III}(R)-(P(C_6H_3-3-$SiMe_3$-2-S)$_3$)]$^-$,[50] e: Ni^{II}($dadt^{Et}$)Ni^{I}(SDmp)-(PPh_3).[51]

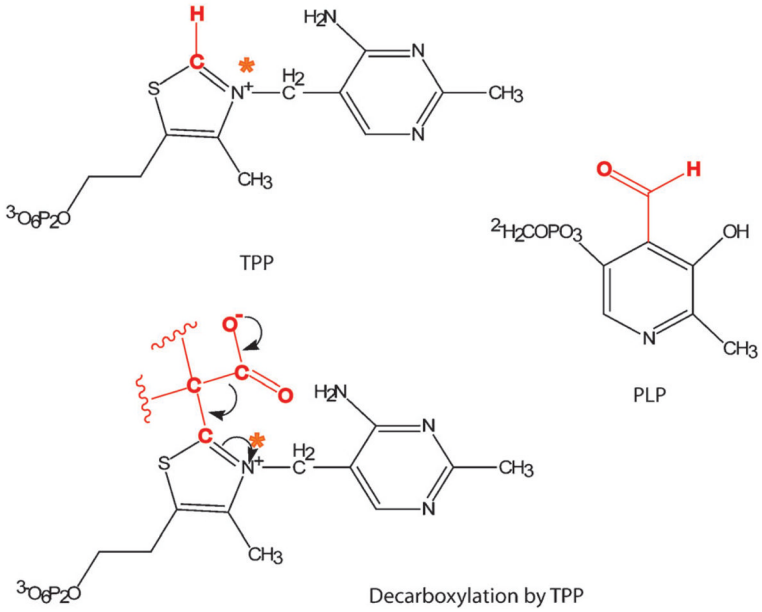

Fig. 6.

The structures of TPP and PLP with the reactive sites highlighted in red. A typical decarboxylation reaction catalyzed by TPP-bound intermediate is also depicted, with the orange star indicating the same nitrogen as on TPP structure.

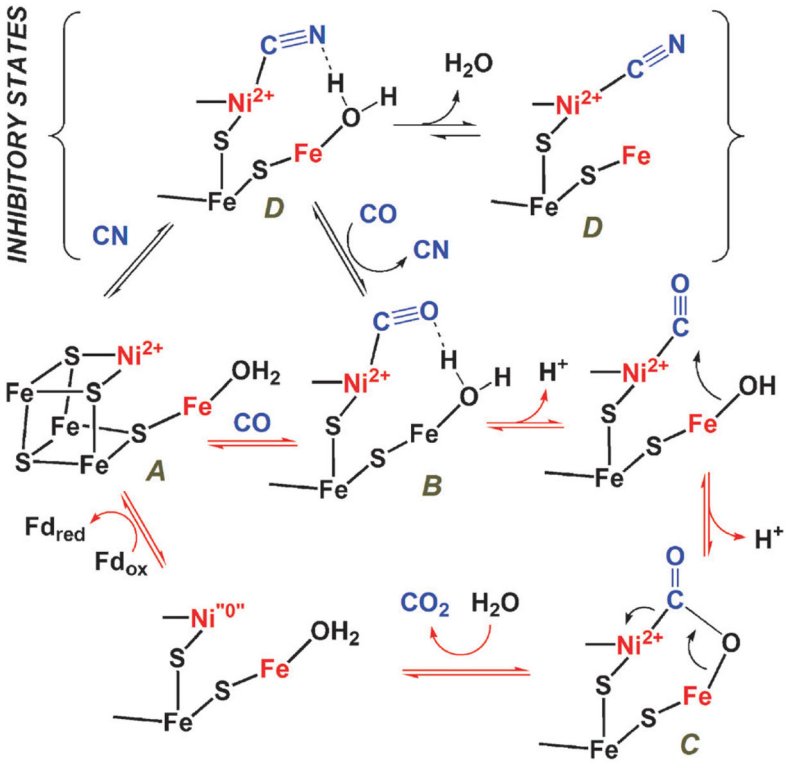

Fig. 7.

Proposed CODH mechanism incorporating the information from recent crystal structures, based on Kung *et al.*, 2010.[141]

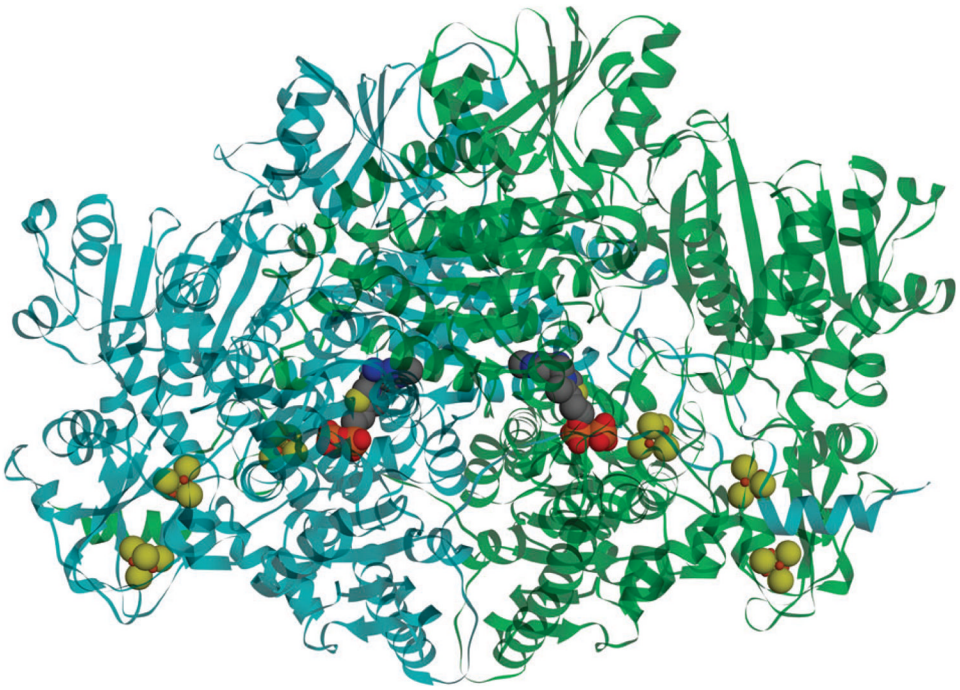

Fig. 8.

The main cofactors and the overall structure of *Desulfovibrio africanus* pyruvate ferredoxin oxidoreductase from pdb:1B0P, shown in sphere and ribbon representation respectively. The enzyme is a homodimer (cyan and green chains), and each monomer contains one TPP and three Fe_4S_4 clusters (spheres).

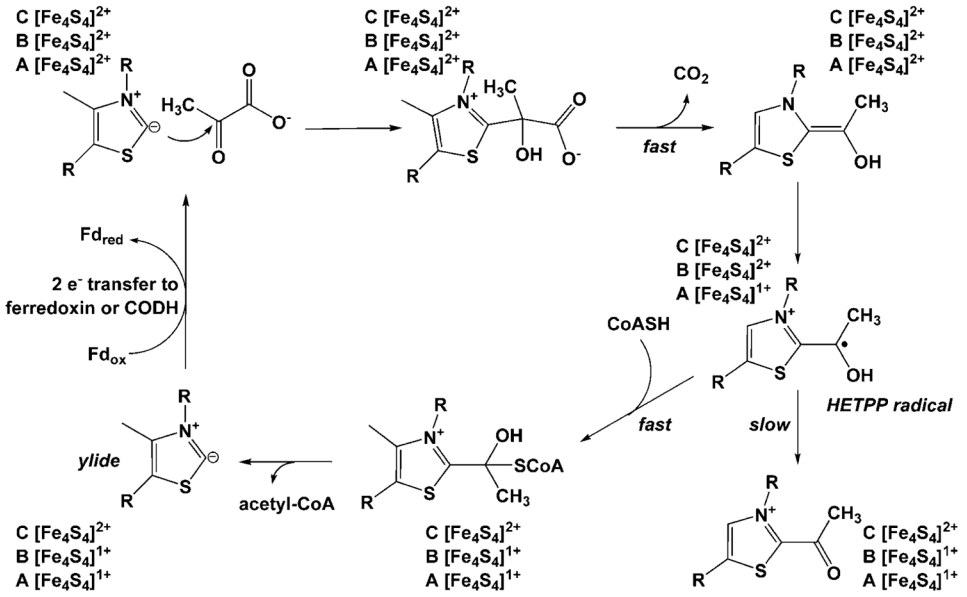

Fig. 9.

PFOR mechanism.[192] See text for further explanation of the steps of the reaction mechanim.

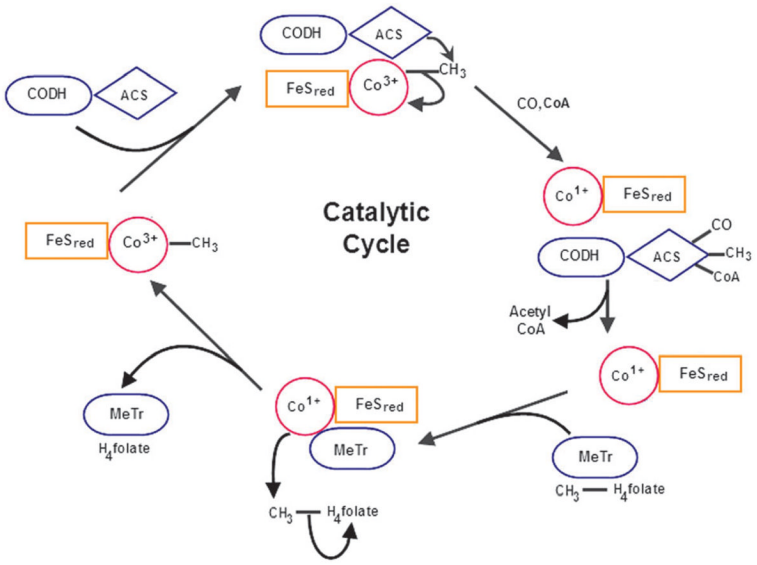

Fig. 10.
The catalytic cycle of CFeSP and its interactions with CODH/ACS and MeTr.

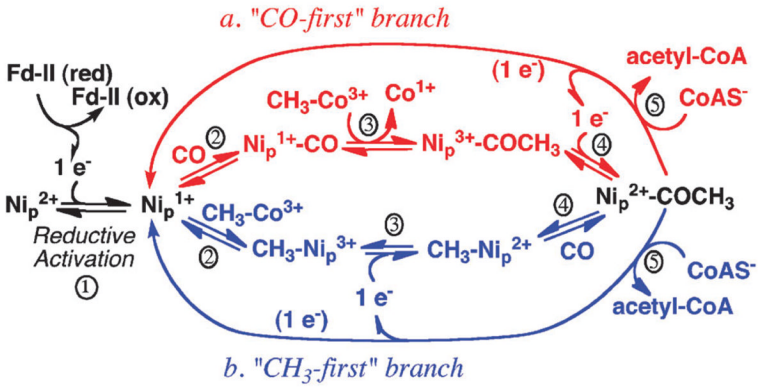

Fig. 11.

The proposed mechanism of acetyl-CoA formation by ACS. CO or the methyl group bind randomly, as shown in path a (red) or b (blue), respectively.

Table 1

Known pathways of CO_2 fixation by microbes

Pathway name	CO_2-fixing enzymes	Examples of Microbes	O_2 sensitivity
Calvin-Benson-Bassham Cycle	RubisCO	Aerobic autotrophic bacteria (cyanobacteria, purple sulfur bacteria… *etc*.)	Tolerant
Reductive tricarboxylic acid cycle	2-oxoglutarate synthase, isocitrate dehydrogenase, pyruvate synthase, PEP carboxylase	Bacteria such as *Chlorobium* sp. and *Desulfobacter* sp.	Sensitive
Reductive acetyl-CoA pathway	Acetyl-CoA synthase, formate dehydrogenase	Methanogenic archaea and acetogenic bacteria	Sensitive
3-Hydroxypropionate/malyl-CoA cycle	Acetyl-CoA carboxylase, Propionyl-CoA carboxylase	Phototrophic bacterium, *Chloroflexus aurantiacus*	Sensitive
3-Hydroxypropionate/4-hydroxybutyrate cycle	Acetyl-CoA carboxylase, Propionyl-CoA carboxylase	Autotrophic Crenarchaeota, Sulfolobales, *Metallospharea sedula*	Microaerobic conditions
Dicarboxylate/4-hydroxybutyrate cycle	Pyruvate synthase, Phosphoenol pyruvate carboxylase	Archaea such as *Ignicoccus hospitalis*, *Thermoproteus neutrophilus*	Sensitive

Table 2

Reactions involving CO and CO_2 as either substrate or product

Reaction type	Cofactor	Examples
Decarboxylation	TPP[55,56]	Phenylpyruvate decarboxylase, pyruvate decarboxylase, pyruvate oxidase, 2-oxoglutarate decarboxylase.
	PLP[78]	Amino acid decarboxylase, ornithine decarboxylase, dialkylglycine decarboxylase.
	Cofactor independent[79]	Acetoacetate decarboxylase.
	Protein-radical[80]	Pyruvate formate lyase.
Carboxylation	Biotin[81,82]	Acetyl-CoA and propionyl-CoA carboxylases, pyruvate carboxylase.
	Metals[82,83]	Acetone carboxylase, ribulose-1,5-bisphosphate decarboxylase (RubisCO), phosphoenolpyruvate carboxylase, isocitrate dehydrogenase, pyruvate synthase, pyruvate carboxylase, acetyl-CoA and propionyl-CoA carboxylases.
	Acetyl-Coenzyme A (strong activator)[84]	Phosphoenolpyruvate carboxylase.
Decarbonylation	Various cofactors[85]	Formation of CO for H-cluster,[57] heme oxygenase, 3-hydroxy-4-oxoquinoline-2,4-dioxygenase, quercetin-2,3-dioxygenase, octadecanal decarbonylase, acireductone dioxygenase, acetyl-CoA decarbonylase synthase
CO as substrate	C-cluster, A-cluster[86]	Carbon monoxide dehydrogenase, acetyl-CoA synthase
CO_2 reduction to Formate and CO, Formate and CO oxidation to CO_2	C-cluster, molybdenum, tungsten, selenocysteine, FMN, Fe–S clusters	Carbon monoxide dehydrogenases, formate dehydrogenases with molybdenum and tungsten, selenocysteine, FMN cofactors, and Fe–S clusters,[63,64] formate dehydrogenases with no prosthetic groups.[65]

Table 3

List of CO-oxidizers.

	Electron acceptor	Autotrophic pathway	CODH	Taxonomic group	Example organisms	Ref.
Methanogenic Archaea	CO_2 reduction to methane	Wood-Ljungdahl	NiFe CODH (IV–V)[a]	Euryarchaea	*Methanosarcina barkeri*, *Methanobacterium formicicum*, *Methanothermobacter thermautotrophicus*	93
Acetogenic bacteria	CO_2 reduction to acetate	Wood-Ljungdahl	NiFe CODH III	Clostridia, deltaproteobacteria, Dehalococcoidetes	*Moorella thermoacetica*, *Clostridium formicicum*	94–96
Purple non-sulfur photosynthesizing bacteria	protons	Calvin cycle	NiFe CODH (I or II)	α-proteobacteria	*Rhodopseudomonas*, *Rhodospirillum rubrum*	97,98
Sulfate reducing deltaproteobacteria	sulfate, sulfite	none	NiFe CODH IV	δ-proteobacteria	*Desulfovibrio desulfuricans*	99–101
Aerobic carboxydobacteria	O_2	Calvin cycle	Mo CODH	Many Gram-negative bacteria	*Oligotropha* (formerly *Pseudomonas*) *carboxydovorans*	71,102
Non-acetogenic clostridia	CO_2 reduction to formate	none	Not known	Clostridia	*Clostridium pasteurianum*	103,104
Plants and algae	O_2	Calvin cycle	cytochrome *c* oxidase	Viridiplantae	*Chlamydomonas reinhardtii*, *Arabidopsis thaliana*	105

[a]The Roman numerals indicate the closest homologue in *C. hydrogenoformans.*